

D2.1 Dataset on carbon sequestration following reforestation and proforestation

Planned delivery date (as in DoA): M12 Due date of deliverable: September 2024

Work Package: WP2

Work Package leader: UNIUD Deliverable leader: UNIUD

CUP number: 2022R7F259

REWILDFIRE — PIANO NAZIONALE DI RIPRESA E RESILIENZA (PNRR)

Missione 4 "Istruzione e Ricerca" - Componente C2

Investimento 1.1, "Fondo per il Programma Nazionale di Ricerca e Progetti di Rilevante Interesse Nazionale (PRIN)"

Project Acronym: REWILDFIRE

Rewilding policies for carbon sequestration under increasing fire risk

Duration of the project: September 28st, 2023 – September 27st, 2025

CITATION:

Piazza N., Foscari A., Tomao A., Alberti G. (2025). D2.1 Dataset on carbon sequestration following reforestation and proforestation. Missione 4 "Istruzione e Ricerca" - Componente C2 Investimento 1.1, "Fondo per il Programma Nazionale di Ricerca e Progetti di Rilevante Interesse Nazionale (PRIN)", Project REWILDFIRE.

ACKNOWLEDGEMENTS



DISCLAIMER

Funded by the European Union and the Ministry of the University and Research. Views and opinions expressed are however those of the author(s) only and do not necessarily reflect those of the European Union. Neither the European Union nor the granting authority can be held responsible for them.

Table of Contents

Ta	ble	of Contents	2
Ex	ecu	tive Summary	4
Ke	ywc	ords	4
Ac	rony	yms	4
De	finit	tions	5
Sc	ope	of the deliverable	6
1.	S	election of experimental sites	7
	1.1.	Afforestation	7
	1.2.	Proforestation	12
2.	C	onsidered carbon pools and protocols	15
3.	Fi	ield survey	16
;	3.1.	Identification of the centre of the plot	16
,	3.2.	Survey of standing trees and stumps	16
;	3.3.	Living and dead standing trees and stumps	17
;	3.4.	Lying deadwood	23
	C	oarse woody debris	23
	Fi	ine woody debris	24
;	3.5.	Fuel Biomass	25
	SI	hrubs and grass	25
	V	ery fine woody debris and litter	28
,	3.6.	Soil survey	29
4.	A	ssessment of the aboveground carbon stock	31
	4.1.	Standing living trees	31
	4.2.	Root biomass of standing living trees	32
	4.3.	Deadwood biomass	32
	St	tanding dead trees	32
	Ві	roken standing dead trees (snags)	33
	C	oarse woody debris	33
	Fi	ine woody debris	33
	St	tumps	33
	В	asic density of deadwood by decay stage	34
	G	rass and shrub biomass	35
	C	arbon content	36
	4.4.	Very fine woody debris and litter	36

REWILD-FIRE – Deliverable 2.1

5. As	Assessment of soil carbon stock		
6. Ma	ain results and discussion	38	
6.1.	Description of the dataset	38	
6.2.	Afforestation	38	
6.3.	Proforestation	46	
7. Re	eferences	54	

Executive Summary

This deliverable is part of the ongoing work under Work Package (WP) 2 and has the following objectives:

- 1) to present the methodology used for data collection, including how afforestation on abandoned agricultural land and proforestation sites were identified; and
- 2) to describe the procedures used to estimate both aboveground and belowground carbon (C) stocks.

Keywords

Rewilding, proforestation, afforestation, land abandonment, forest succession, carbon stocks

Acronyms

IGM: Istituto Geografico Militare

ISTAT: Istituto nazionale di statistica

AGB: Aboveground Biomass

DBH: Diameter at breast height (1.30 m)

GA: Grant Agreement

UNITO: University of Torino (Italy)

UNIUD: University of Udine (Italy)

UNIMI: University of Milano (Italy)

Definitions

Afforestation: the natural process through which a forest expands into previously non-forested land.

Landscape: a 50-150 km² tract of land situated within the same ecoregion.

Patch: a homogeneous area of the landscape that contrasts with its surroundings—in this case, distinguished by its age of formation.

Proforestation: the suspension of active forest management to permit the forest's spontaneous, natural development.

Basic wood density (σ): the weight of a dried wood sample divided by the fresh wood sample volume, expressed in g cm⁻³ (Bitunjac et al. 2023).

Carbon Stock: the absolute quantity of carbon held within a pool at a specified time (MgC ha⁻¹) (IPCC, 2000).

Chronosequence: a series of sites that differ in age or time since abandonment, but otherwise occur on similar soil types and environmental conditions within the same climatic zone (Chazdon, 2013; De Palma et al., 2018). Chronosequences, by assuming space-for-time substitution, are used to infer temporal dynamics from measurements at sites of different ages, but similar land-use histories.

Forest Stand: a community of trees, including aboveground and below-ground biomass and soils, sufficiently uniform in species composition, age, horizontal and vertical structure, and environmental conditions to be managed as a unit (IPCC, 2006, 2003).

Forest structure: horizontal and vertical distribution of layers and attributes in a forest including the trees, shrubs, and ground cover (Gadow et al., 2012).

Forest category: a category of forest defined by its composition and/or site factors (locality), as categorised by each country in a system suitable to its situation (EEA, 2007).

Land abandonment: process whereby human control over land (e.g., agriculture) is given up and the land is left to nature.

Plant biodiversity: variety and variability of plant life within a specific area or ecosystem.

Plot: portion of a site within which stand and/or soil data are collected and that is considered representative of that specific site.

Sampling unit: sampling element or point within a plot (i.e., a tree, a soil sampling point, etc.).

Secondary forests: forest or woodland area which has regenerated through largely natural processes after human-caused disturbances or equivalently disruptive natural phenomena (Chokkalingam and De Jong, 2001).

Site: homogenous area in terms of environmental conditions, land use (forest or agriculture) and time since abandonment.

Time since abandonment: time in years since forest management has stopped (proforestation) or agricultural use has been abandoned (afforestation).

Scope of the deliverable

Work Package 2 (WP2) of the REWILDFIRE project focuses on investigating carbon balance dynamics following afforestation of abandoned agricultural land and proforestation processes, using empirical data collected from experimental sites across the Alpine region. Under Task 2.1, field surveys were conducted within selected chronosequences using circular plots (513 m²), in accordance with the Italian National Forest Inventory (INFC) protocol, to quantify aboveground carbon (C) stocks among the aboveground compartment (i.e., standing trees). To assess C stocks in the litter, deadwood, grasses and shrubs as well as in soil standardized sampling protocols were developed and agreed among project partners.

Each selected experimental area included one or more chronosequences (replicates), representing different stages of natural succession following agricultural or forest management abandonment (i.e., varying times since abandonment, TSA). The aboveground data collected - including measurements of individual trees and lying deadwood - were used by project partners to calculate C stocks in the different ecosystem pools at the site level. This information provides the empirical foundation for modelling C dynamics (D2.2) associated with rewilding processes targeted by the REWILD-FIRE project.

This methodology for the field sampling of standing trees and deadwood as well as C stock calculations was discussed, harmonized and shared with the EU-funded WILDCARD project (www.wildcard-project.eu) coordinated by University of Udine, which investigates similar rewilding processes at the European scale.

1. Selection of experimental sites

1.1. Afforestation

The REWILDFIRE project focuses on four Italian ecoregions within the Alpine arc, as defined by ISTAT (Figure 1; https://www.istat.it/it/archivio/224780) (Figure 1):

- 1A1b Divisione Temperata, Provincia Alpina, Sottosezione Alpi Nord-Occidentali
- 1A2c Divisione Temperata, Provincia Alpina, Sottosezione Alpi Nord-Orientali
- 1A2a Divisione Temperata, Provincia Alpina, Sottosezione Prealpina
- 1A2b Divisione Temperata, Provincia Alpina, Sottosezione Dolomitico-Carnica

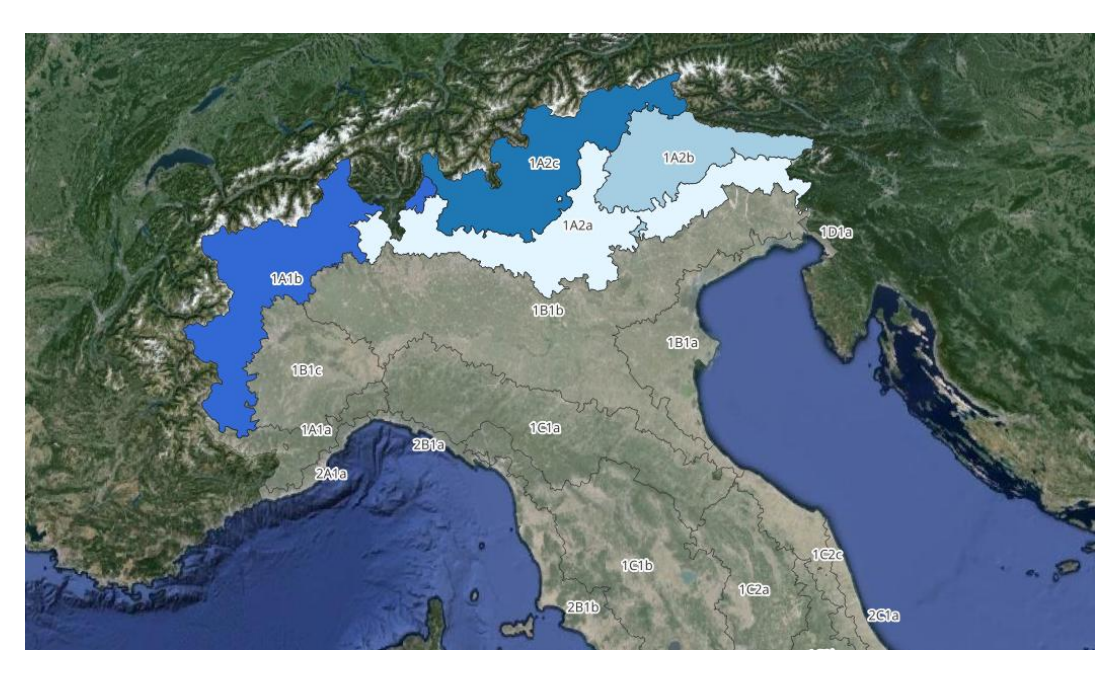


Figure 1. Map of Italian ecoregions according to ISTAT. The four ecoregions in this study are highlighted.

Within each ecoregion (Figure 2), the study areas - referred to as "landscapes" - are defined as environmentally homogeneous zones of approximately 150 km². These landscapes were selected within the municipalities where afforestation was the main land use change according to Corine Land Cover maps. In each selected landscape, two land-use transitions were considered by the project: (1) the land use change from cultivated land to forest, and (2) the shift from meadow/pasture to forest. These transitions were replicated across three chronosequences (replicates), each consisting of five time since abandonment (sites).

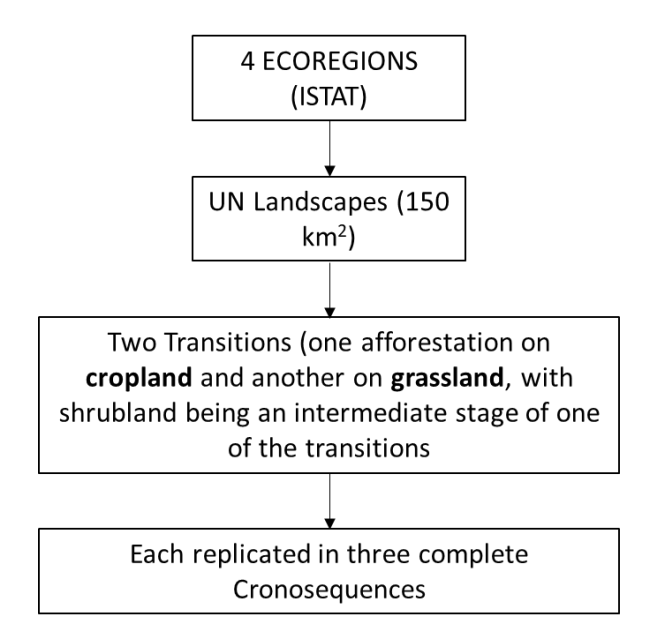


Figure 2. Scheme of the experimental design for natural afforestation.

The three chronosequences within each landscape were selected within a limited area characterized by similar environmental conditions using aerial photographs. Some of these images - such as the 2000s orthophotos - were already orthorectified and georeferenced and were available through the national or individual regional geoportals. Where such data were not accessible, images were requested or purchased from official providers, such as the Istituto Geografico Militare (IGM; https://www.igmi.org/it/geoprodotti#b start=0). In these cases, georeferencing was performed using the "Georeferencer" tool in QGIS (QGIS Development Team). An initial, approximate georeferencing was sufficient to identify areas of interest where land-use changes were evident. This was followed by more precise georeferencing using the "Thin Plate Spline" transformation algorithm, with Ground Control Points (GCPs) placed specifically within the areas of interest. Although this method does not correct for elevation-induced distortions (i.e., orthorectification), it proved sufficiently accurate for detecting land-use transitions over small areas. Thus, each chronosequence comprised five chronological phases (sites), covering a temporal range of approximately 20 years each:

- Grassland or cropland as of 2020
- Forest established between 2000 and 2020
- Forest established between 1980 and 2000
- Forest established between 1954 and 1980
- Forest already forest in 1954

Following georeferencing, the next step was to identify areas that underwent land-use change - from grassland, cropland, or meadow to forest - within the time span between two consecutive image sets. To assign different land-use categories, we started from the landscape patterns visible in the oldest available orthophoto (1954), considering the following aspects:

- **Cropland:** areas characterized by highly geometric plot shapes and notable colour heterogeneity (Figure 3).
- **Grassland:** identified as treeless areas with minimal signs of human impact. In the case of mown grasslands, these may resemble agricultural land but typically feature more elongated plot shapes and more uniform coloration (Figure 4).





Figure 3. Agricultural landscape under cultivation in 1954, Valle di Soffumbergo and Raschiacco (Udine Province)





Figure 4. Grassland and mowed areas in 1954 in Valle di Soffumbergo (UD - left) and Canebola (UD - right).

Based on multi-temporal orthophotos, polygons were delineated to represent different age classes within each land-use category. The survey plots were then randomly positioned within these polygons. Below is an example illustrating the transition from cultivation to forest between 1954 and 1978 (Figure 5) and the final results after interpretation of all the available photos (Figure 6).

REWILD-FIRE – Deliverable 2.1

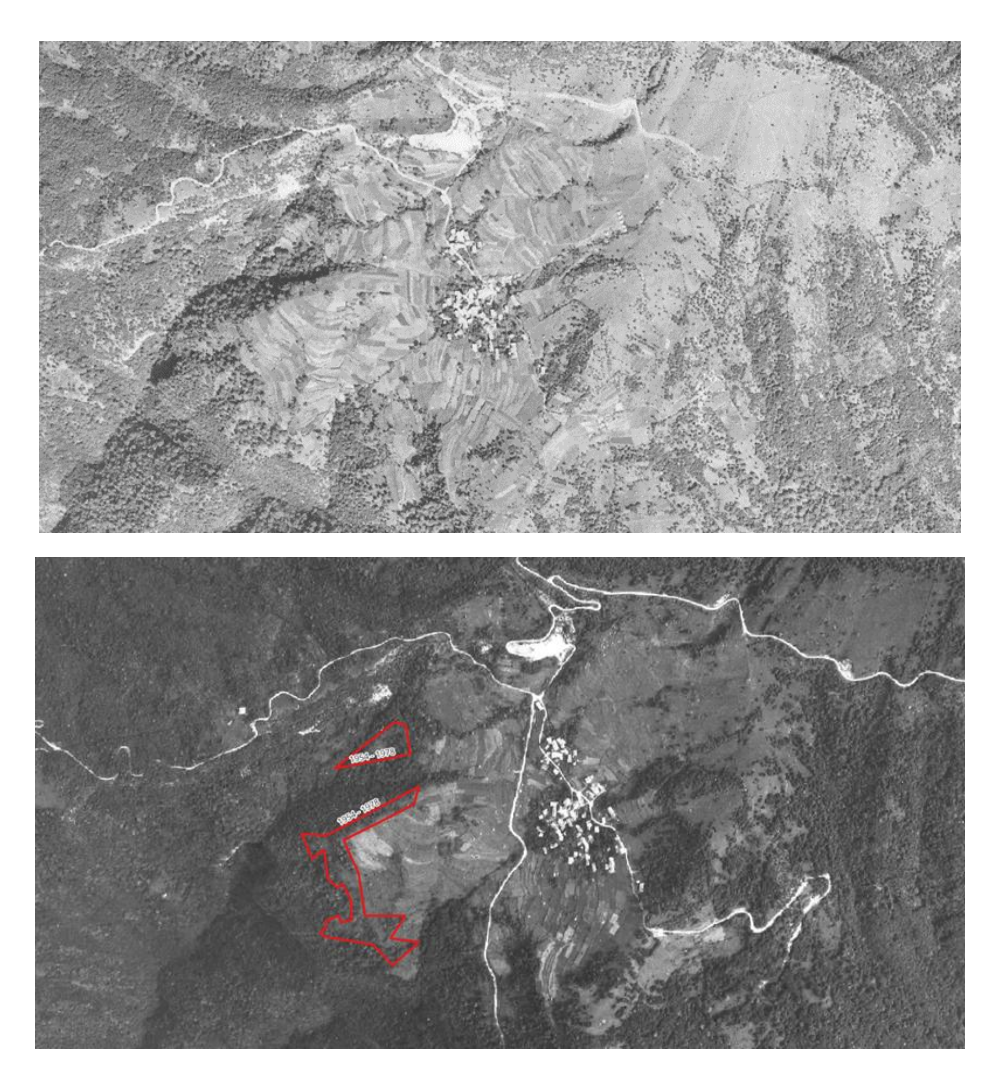


Figure 5. Valle di Soffumbergo, Faedis (UD); orthophotos from 1954 (above) and 1978 (below). The red polygon indicates the area that underwent land-use change (forest expansion).

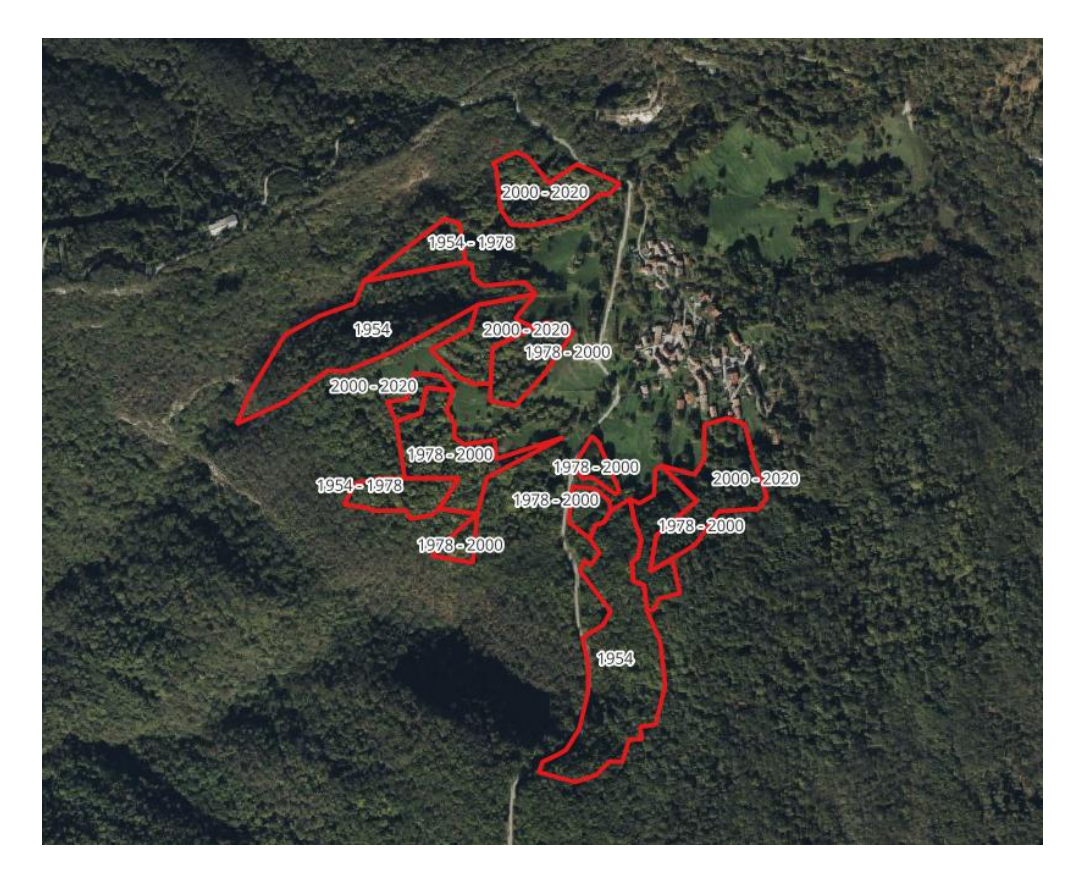


Figure 6. Polygons indicating land-use changes over different time periods in the Soffumbergo Valley (UD).

The analysis of land-use transitions within the selected landscapes led to the identification of numerous forest polygons of varying age classes, which served as the basis for potential chronosequences. For the class representing grassland or cropland in 2020 - the starting point of the chronosequence - current grasslands or croplands were considered, provided they had maintained the same land use since 1954. In the case of croplands, due to the difficulty of finding plots still under cultivation today, areas that remained cultivated at least until 2000 were also included. Sampling plots for vegetation and soil surveys were established within each site following on-the-ground verification of the area's suitability for the project's objectives and considering only forest stands which have not been subject to any anthropogenic disturbance or logging since their establishment.

Table 1 presents the distribution of chronosequences and sites among the project partners. In total, 120 sites were sampled across the study design (4 ecoregions \times 1 landscape \times 2 landuse transitions \times 3 chronosequences \times 5 sites).

	Ecoregion	Landscape	Chronosequences (n. replicates)	Transitions	Age classes (including crops or meadows)	Ecoregion Code	n. sites (total)
PIEMONTE	D	1	3	Grassland	5	1A1B	15
(UNITO)		2	3	Cropland	5	1A1B	15
LOMBARDIA	С	1	3	Grassland	5	1A2C	15
(UNIMI)		2	3	Cropland	5	1A2C	15
	А	1	4	Grassland	5	1A2A	20
FVG		2	3	Cropland	5	1A2A	15
(UNIUD)	В	1	3	Grassland	5	1A2B	15
		2	3	Cropland	5	1A2B	15
						TOTAL	125

Table 1. Number and regional distribution of the project's experimental design elements

1.2. Proforestation

To analyse proforestation dynamics - the natural development of a forest following the abandonment of active management - case study landscapes were selected within predominantly forested areas. Within each landscape (as previously defined), three forest stands were chosen, each representing one of the following management abandonment classes:

- Currently managed forest (last intervention within the past 10 years).
- Abandonment within the past 25–50 years (last intervention between 25 and 50 years ago);
- Abandonment of forest management over 50 years ago (last intervention >50 years);

Each selected stand was required to meet the following criteria:

- 1. Belong to the dominant forest type of the corresponding ecoregion;
- 2. Share the same silvicultural system across all three temporal classes (e.g., coppice, abandoned coppice; transitional high forest; high forest);
- 3. Exhibit similar site conditions (e.g., elevation, aspect).

The two abandonment classes were identified using forest management plans and harvesting records to confirm the cessation of silvicultural activities and to determine the date of the last intervention. The currently managed forests were either high forests or mature coppices at the end of their rotation period, just prior to seed cutting or coppicing.

Within each forest stand representing one of the three abandonment classes, three sampling plots were established for soil and vegetation surveys (Table 2). These plots were arranged in an equilateral triangle, with each plot located 35 meters from the centroid, which coincides with the centre of the selected forest polygon (Figure 7).

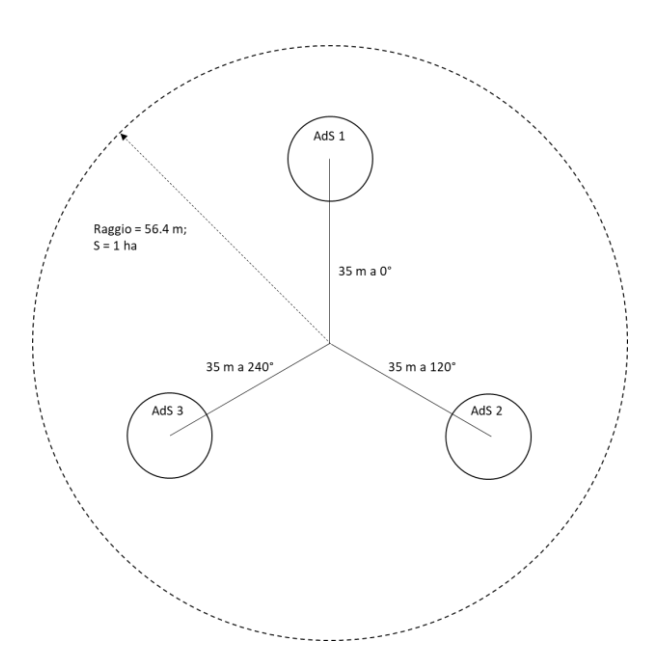


Figure 7. Layout of sampling plots in proforestation sites.

In total, 36 areas were surveyed (4 eco-regions x 1 landscape x 3 abandonment classes x 3 replications (plots)) Table 2.

Table 2. Distribution of managed and proforested plots among the different ecoregions included in the project.

	Ecoregion	Code	Age classes	N. plots	n. sites (total)
PIEMONTE (UNITO)	D	1A1B	3	3	9
LOMBARDIA (UNIMI)	C	1A2C	3	3	9
FVG	А	1A2A	3	3	9
(UNIUD)	В	1A2B	3	3	9
				TOTAL	36

All areas identified for both afforestation and proforestation are shown in Figure 8.

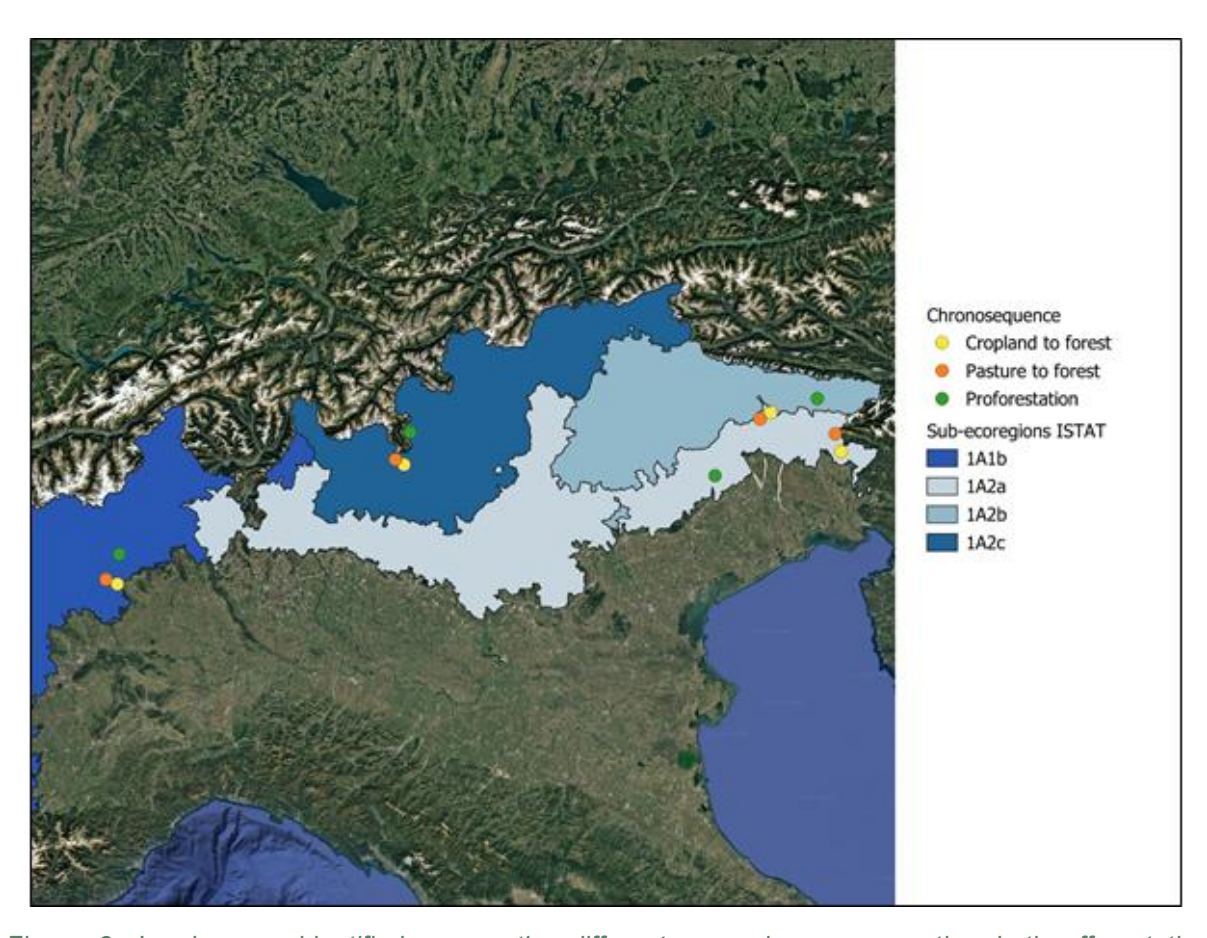


Figure 8. Landscapes identified across the different ecoregions representing both afforestation (cropland to forest and pasture to forest) and proforestation processes.

2. Considered carbon pools and protocols

For the purposes of the REWILDFIRE project, the following C pools identified by the IPCC guidelines have been considered (Figure 9; IPCC, 2006):

- 1. **Living trees**: this pool includes the living biomass of the above ground (stems, branches, leaves) and roots (plants with dbh > 4.5 cm);
- 2. **Shrubs**: this pool includes the living biomass of the understory (stems, branches, leaves) and roots (plants with dbh < 4.5 cm)
- 3. **Grass** (only for meadows and pastures): this pool includes the living biomass of the herbaceous layer including roots.
- 4. **Standing deadwood**: this pool includes standing dead trees, branches and roots (plants with dbh > 4.5 cm);
- 5. **Stumps**: this pool includes the biomass of stumps and their roots
- 6. **Lying Dead wood**: this pool includes the biomass of all woody residues lying on the ground. In particular, we distinguish between coarse woody debris (diameter greater than 10 cm), fine woody debris ($2.5 \text{ cm} \le \text{diameter} < 10 \text{ cm}$) and very fine woody debris (diameter < 2.5 cm).
- 7. **Litter**: this pool includes fresh litter (OL horizon), i.e. leaves, fruits still undecomposed.
- 8. **Soil:** this pool includes both organic and mineral layer.

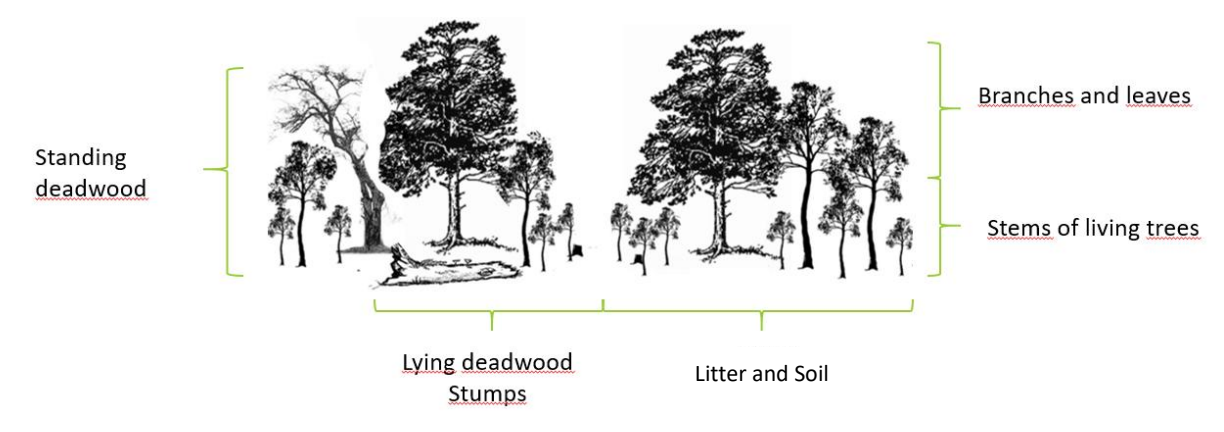


Figure 9. Scheme of the carbon pools considered in the project

3. Field survey

3.1. Identification of the centre of the plot

Once reached the survey point, the centre of each plot was permanently marked using a picket in order to guarantee its identification over time, at least for the duration of the project. We used tear-proof X-GRIP pickets measuring 360 mm in galvanized steel, shaft ø 15mm, white-red plasticized from Eurotec SNC of Parma (Figure 10). The exact position of the centre was recorded with GNSS with sub-metric precision.

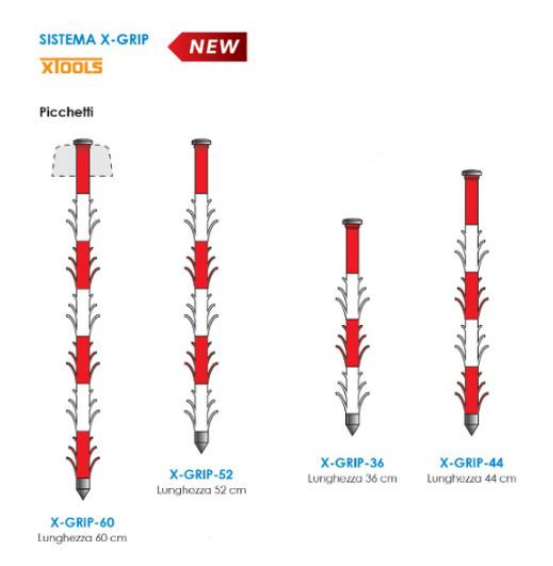


Figure 10. Eurotec snc X-GRIP picket to permanently identify the central point of the PLOT 13

3.2. Survey of standing trees and stumps

After the identification of the centre of the plot and before proceeding with the dendrometric measurements, the operator proceeded with a qualitative description of the stand considering the following characteristics and filling out the plot survey form:

ATTRIBUTE	DATA_TYPE	DESCRIPTION
INSTITUTE	CHAR	Name of institution (abbreviation)
CHRONO_ID	CHAR	Chronosequence ID
SITE_ID	CHAR	Site ID within the chronosequence
TIME_SINCE_ABANDONEMEN T	INTEGER	Age since age of establishment (this can be derived by multi-temporal aerial photos)
PLOT_ID	INTEGER	Unique plot ID within the site
LARGE_PLOT_R	INTEGER	Radius of large plot used for censusing trees with DBH ≥ 10 cm
SMALL_PLOT_R	INTEGER	Radius of small plot used for censusing trees with 4 ≤ DBH < 10 cm
FOREST_TYPE	CHAR	Forest type according to the European classification
VERTICAL_STRUCTURE	CHAR	Vertical structure (single-layer, two-layered, multi-layered)

HORIZONTAL_STRUCTURE	CHAR	Horizontal structure (random, regular, grouped)
COVERAGE	CHAR	Coverage (regular, full, incomplete, poor)
MANAGEMENT_TYPE	CHAR	Management type (high forest, coppice, temporary high forest [i.e. conversion from coppice to high forest], not determinable)
RECENT_MANAGEMENT	BOOL	Signs of recent silvicultural practices (yes, no)
ASPECT	INTEGER	Main aspect of the plot expressed in degrees from north (0-360)
SLOPE	DECIMAL	Average slope of the plot (expressed in %)
COORDINATES_N	DECIMAL	Coordinate of the center of the plot in ETRS89/extended LAEA Europe (EPSG:3035) coordinate system (https://epsg.io/3035)
COORDINATES_E	DECIMAL	Coordinate of the center of the plot in ETRS89/extended LAEA Europe (EPSG:3035) coordinate system (https://epsg.io/3035)

3.3. Living and dead standing trees and stumps

Two concentric circular plots were identified on the horizontal plane through the use of the Vertex hypsometer in distance meter mode (see Figure 11). The larger plot was a circle with a radius of 13 m (area of 500 m²; PLOT_13). The smaller concentric plot had a radius of 4 m (area of 50 m²; PLOT_4). Within the PLOT_13 all trees with the DBH greater than or equal to 10 cm were measured, while within the PLOT_4 all trees with a diameter between 4 and 10 cm were measured.

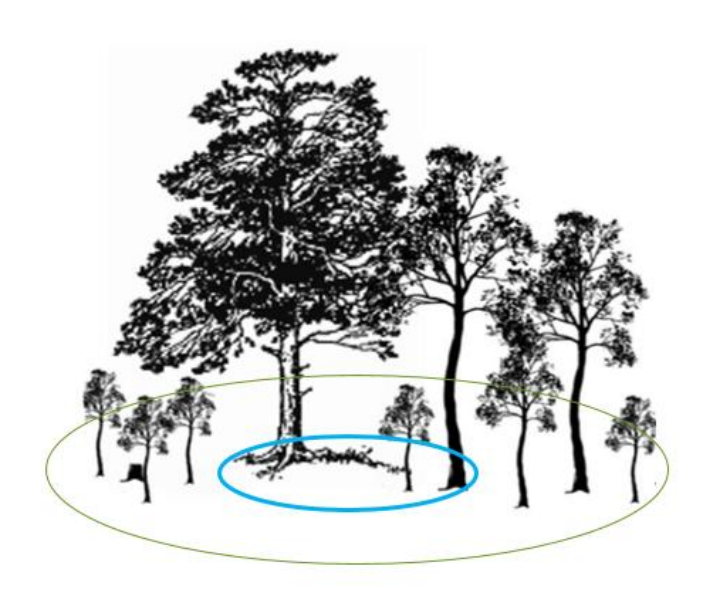


Figure 11. Example of concentric plots: the PLOT_13 in green; the PLOT_4 in blue

For each sampled tree, the following information was recorded on the appropriate survey form:

	- · - · - · / - ·		
ATTRIBUTE	DATA TYPE	UNITS	OBLIGATION
INSTITUTE	CHAR	NA	mandatory
CHRONO_ID	CHAR	NA	mandatory
SITE_ID	CHAR	NA	mandatory
PLOT_ID	INTEGER	NA	mandatory
TREE_ID	INTEGER	NA	mandatory
STEM_ID	INTEGER	NA	mandatory
MULTI_STEM	ENUM	NA	mandatory
LIFE	ENUM	NA	mandatory
MORT_MOD	ENUM	NA	mandatory
SPECIES	VARCHAR	NA	mandatory
DBH	INTEGER	cm	mandatory
HOM	DECIMAL	m	optional, standing only
HEIGHT	DECIMAL	m	optional for standing trees, mandatory for snags and stumps
DECAY	ENUM	NA	mandatory, dead only
AGE	INTEGER	NA	optional
COORD_X	DECIMAL	m	optional
COORD_Y	DECIMAL	m	optional
COORD_Z	DECIMAL	m	optional

INSTITUTE – Name of institution (abbreviation)

 $\textbf{CHRONO_ID} - \textbf{Chronosequence ID}$

SITE_ID – Site ID within the chronosequence

PLOT_ID – Unique plot ID within the site

TREE_ID –Unique identifier of the tree individual in the site/plot from the database perspective. A tree may have one or more stems.

STEM_ID – Distinct identifier for individual stems within one tree, separated up to a height of 1.3 meters (for more see MULTI_STEM). For single stem STEM_ID = 1, for multi-stemmed trees the range is 1:n.

For a schematic representation see Figure 12.

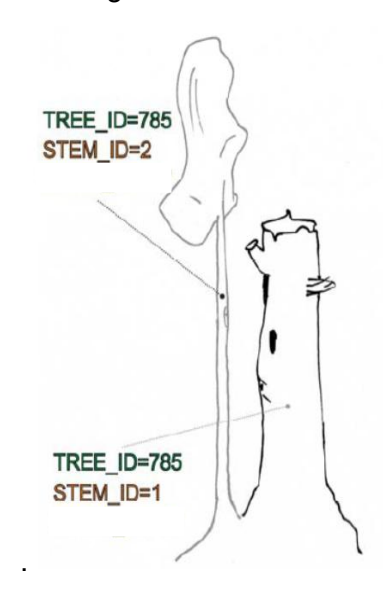


Figure 12. Example of ID coding.

MULTI_STEM – value identifying stem multiplicity within single tree following the classification:

MULTI_STEM	DESCRIPTION
SGL	Single. One stem per one tree individual (Figure 13)
FRK	Forked. Stems branching at a height of 0-1.3 m above the ground; there is one tree-base on the ground (Figure 14).
PLC	Polycormic. Stems of one biological individual, originally shoots resulted from coppicing mainly, but for some broadleaves (e.g. linden) also of natural origin. (Figure 14)
MTR	Mother tree. A lying tree, which is still alive (possibly rooting along the stem), produces measurable orthotropic shoots growing from it (Figure 14).
MTX	From mother tree. Shoots with orthotropic growth originating from the mother tree (Figure 15).

REWILD-FIRE – Deliverable 2.1

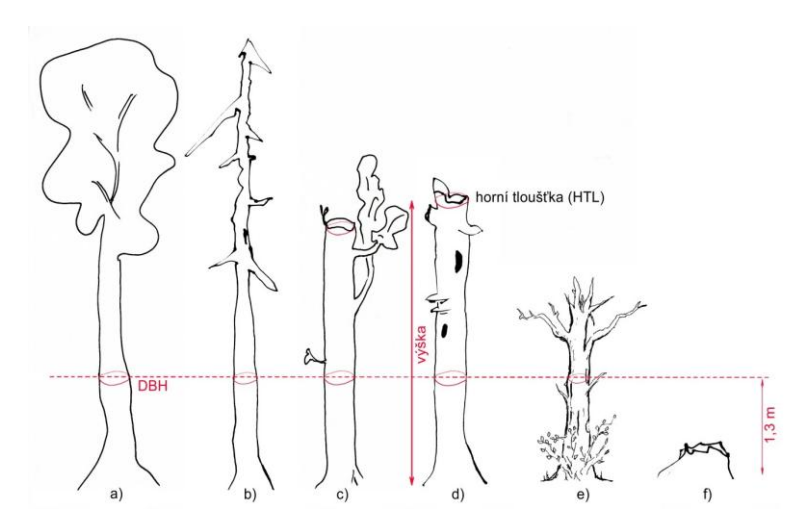


Figure 13. Single stems

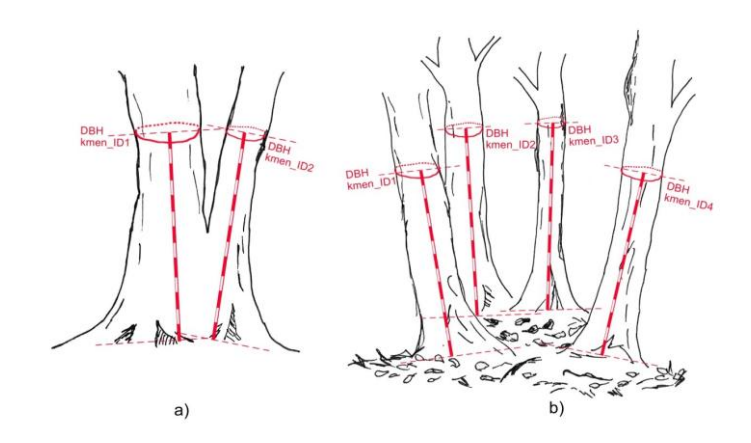


Figure 14. a) Forked, b) Polycormic.

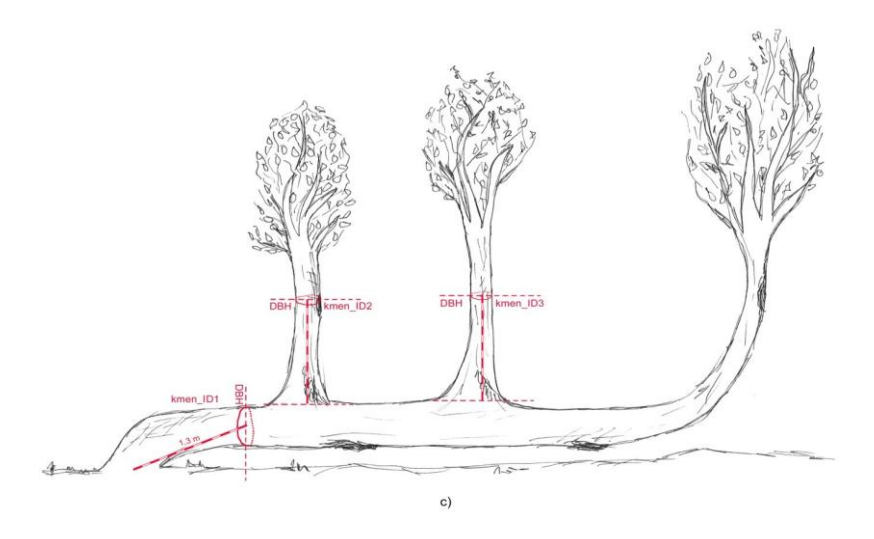


Figure 15. Mother tree (MTR) and shoots from mother tree (MTX).

LIFE - Stem is alive (A) or dead (D).

MORT_MOD - Mortality mode, type of tree death:

MORT_MOD	DESCRIPTION
Uprooted	At least a part of the root system has been torn out of the ground.
Stump	Stem broken at a height < 1.3 m above the ground.
Artificial stump	Stem cut at a height < 1.3 m above the ground.
Break	Stem broken at a height > 1.3 m above the ground.
DALB	Dead Above Alive Below. Tree is live at a height < 1.3 m, but at a height ≥ 1.3 m is dead.
Withered	Standing dead complete stem (died standing).
NA	Living tree.

SPECIES – Six-character abbreviation derived from scientific name

DBH – Diameter at breast height (1.3 m) in cm. Measured by tape preferably rather than caliper. In the case of stumps, in correspondence with the upper section, the two diameters will be measured crosswise and averaged.

HOM – Height of (DBH) measurement. Default is at 1.3 m above the ground. Important when HOM significantly deviates from breast height because of stem malformations. Figure 16.

HEIGHT – Height of the tree or snag, in meters with one decimal place. In the case of stumps, the height from the ground of the upper section (i.e where diameter is measured) will be measured.

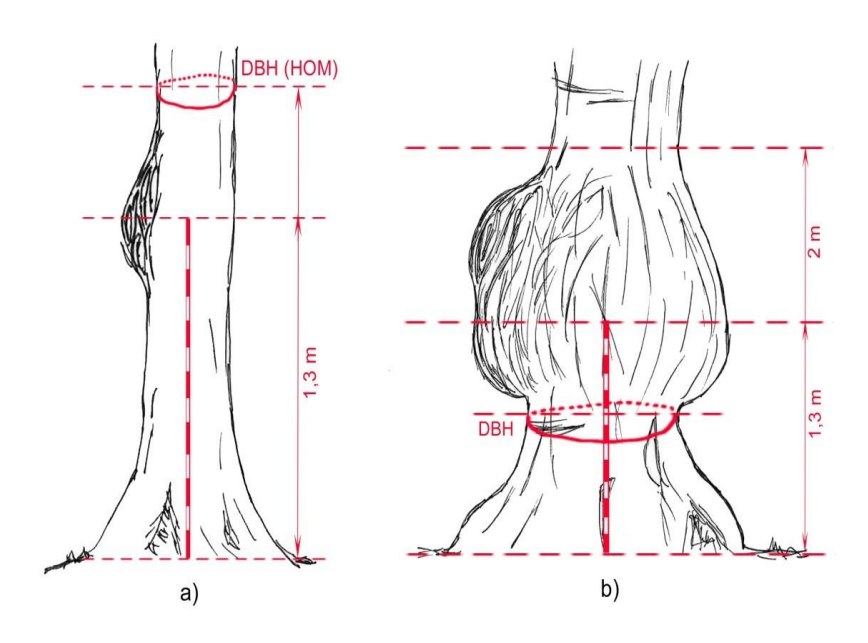


Figure 16. Types of HOM on stem with bulge.

DECAY – Numerical value of the decay class (Figure 17):

SNAG DECAY CLASS	DESCRIPTION
1	Freshly dead (0-5 years for many species); branches of 3rd order are present; the full height of stem is present unless there was damage prior to the mortality event or caused during the mortality event; fully barked (usually ≥80 % of stem surface). The species is still recognizable;
2	Branches of the first order are present; full tree height unless there was damage prior to or during the mortality event; partly barked - usually <80 % of stem surface, broadleaved trees should be still fully barked; the species can usually still be identified;
Only short basal rests of main branches; full height unless there was damage p mortality event; bark missing or absent (usually ≤20 % of stem surface) in the coniferous species;	
4	No branches or small basal rests; height ≤80 % of height curve (according to DBH);
5	Stumps or short snags; the wood is at a stage of advanced rot.

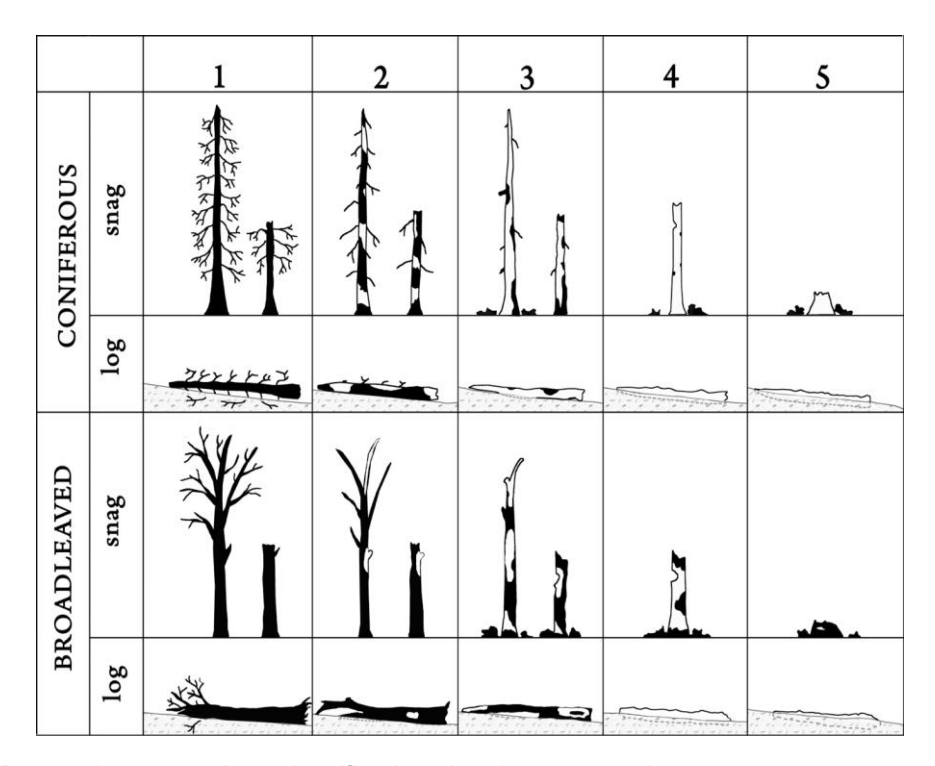


Figure 17. Decay classes. 5-class classification visual representation.

AGE – Age of the tree.

 $\begin{tabular}{ll} \textbf{COORDS}-Tree coordinates, if measured, in ETRS89/extended LAEA Europe (EPSG:3035) coordinate system ($\text{https://epsg.io/}3035$). \end{tabular}$

3.4. Lying deadwood

Coarse woody debris

Measurement of downed coarse woody debris (diameter \geq 10 cm) followed the same method as the measurement of standing stems. Therefore, a full census was conducted on PLOT_13 of all pieces of coarse woody debris with a lower end diameter exceeding the threshold of 10 cm and a length exceeding 1.0 m. Additionally, the upper end diameter, that is within the plot, was measured. Each lying stem coarse woody debris was classified into a decay class and its species was identified, when possible. In case species was not identifiable, at least, deciduous/coniferous categories were reported. This method provided accurate data on coarse woody debris, which represents the largest proportion of dead biomass. Volume of lying stem was determined using the two measured diameters and length:

ATTRIBUTE	DATA TYPE	UNITS	OBLIGATION
INSTITUTE	CHAR	NA	mandatory
CHRONO_ID	CHAR	NA	mandatory
SITE_ID	CHAR	NA	mandatory
PLOT_ID	INTEGER	NA	mandatory
PIECE_ID	CHAR[1]	NA	mandatory
DIAM_LOW	INTEGER	cm	mandatory
DIAM_UP	INTEGER	cm	mandatory
LENGTH	DECIMAL	m	mandatory
DECAY	ENUM	NA	mandatory
GROUND_CONT	BOOLEAN	NA	mandatory
DATE	DATE (YYYY-MM-DD)	NA	mandatory

DIAM_LOW – Lower (wider) diameter of piece of lying log in cm.

DIAM_UP – Upper (thinner) diameter of piece of lying log in cm.

LENGTH - Length of piece of standing snag in m rounded to one decimal digit.

DECAY – Numerical value of the decay class:

LOG DECAY CLASS	DESCRIPTION
1	Freshly fallen dead tree (usually windthrow or a basal rot); wood intact; branches of 2nd order are attached; fully barked (usually ≥80% of stem surface); species is still recognizable;
2	Wood intact to partly hard or soft; branches of first order are partly attached; partly barked; the species can usually still be identified;
3	Wood hard but in large pieces; the wood is not compact any more along the entire stem length with the core or outer mantle subjected to rot. The genus can often be recognized, but species identification is difficult;
4	Wood chunks small, soft, and blocky; the wood is not compact and the cross-section is either elliptical or circular; results in stem breakage, there are often just "little graves" with the patchy vegetation.
5	The wood is at a stage of advanced rot; wood chunks soft and powdery; deadwood no longer has a cylindrical shape; the species cannot be identified any more, a kick into a stem

GROUND_CONTACT – Ground contact of the lying log. Identifies suspended (hanging) logs. Piece of log is assessed as a whole:

VALUE	DESCRIPTION		
1	A piece of the log is in contact with the ground > 50% of its length (Figure 18)		
0	A piece of the log is in contact with the ground < 50% of its length. (Figure 18)		



Figure 18. (a) Ground_cont 0. (b) Ground_cont 1 prevail. (c) Ground_cont 1.

DATE – Date of measurement as YYYY-MM-DD.

Fine woody debris

The survey of fine woody debris (diameter $2.5 \text{ cm} \le x < 10 \text{ cm}$) was carried out according to the line intercept method proposed by Harmon et al. (1996) along three linear transects of 10 m. Such transects were placed in the plot as an equilateral triangle as shown in Figure 19.

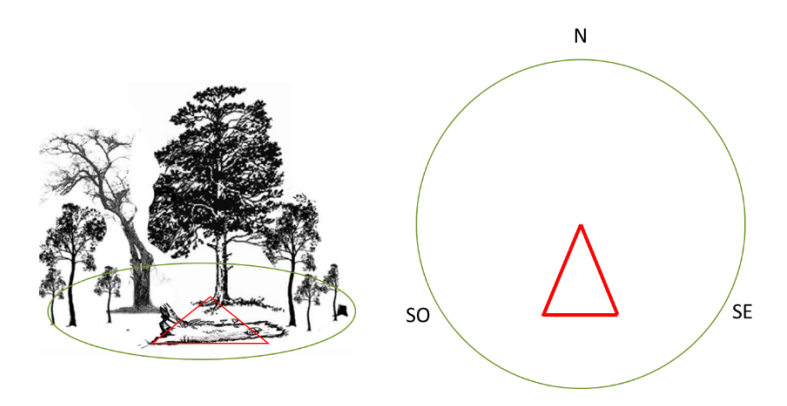


Figure 19. Identification of the transects (red) for laying woody debris survey within the plot

The equilateral triangle was materialized with a 30 m tape using the centre of the plot as the top vertex and then positioning the linear transects one after the other moving clockwise. The diameter of all pieces of dead wood with a diameter ≥ 2.5 cm intersecting each transect was measured. The decay class was determined according to the scale reported for coarse woody debris.

ATTRIBUTE	DATA TYPE	UNITS	OBLIGATION
INSTITUTE	CHAR	NA	mandatory
CHRONO_ID	CHAR	NA	mandatory
SITE_ID	CHAR	NA	mandatory
PLOT_ID	INTEGER	NA	mandatory
TRANSECT_ID	INTEGER	NA	mandatory
PIECE_ID	CHAR[1]	NA	mandatory
DIAM	INTEGER	cm	mandatory
DECAY	ENUM	NA	mandatory

TRANSECT_ID – transect ID within the plot (from 1 to 3)

DIAM – diameter of piece of fine woody debris intersecting the transect in cm.

DECAY – Numerical value of the decay class:

LOG DECAY CLASS	DESCRIPTION		
1	Freshly material; fully barked (usually ≥80% of stem surface); species is still recognizable;		
2	Wood hard but in large pieces; the wood is not compact any more along the entire stem length with the core or outer mantle subjected to rot. The genus can often be recognized, but species identification is difficult;		
3	The wood is at a stage of advanced rot; wood chunks soft and powdery; deadwood no longer has a cylindrical shape; the species cannot be identified any more, a kick into a stem		

3.5. Fuel Biomass

Shrubs and grass

Fuel biomass of shrubs and grass were assessed along the three linear transects of 10 m used for fine woody debris (Figure 19). Every 2 meters along each of the three 10-meter transects, the operator placed a folding meter stick vertically on the ground. At each point, the operator recorded whether fuels from the various fuel classes were in contact with the stick, thereby determining their presence or absence at that specific location along the transect. If the fuel of class j did not touch the stick at point i, it was recorded as "absent"; otherwise, it was recorded as "present." The operator also recorded the presence or absence of rock and bare soil at each point.

After recording the presence or absence of each fuel class, the operator measured the maximum height (in cm) from the ground reached by each identified fuel class (Figure 20).

The considered types classes were the following:

- Litter:
- Grass (Gr);
- Shrub (Sh)¹.

¹ Shrub with a diameter at breast height <4cm

For shrubs, the operator was also required to record the scientific name of the shrub species (e.g., *Calluna vulgaris*). The survey methodology described here enabled the calculation of the percent coverage of different fuel categories, which in turn allowed for the estimation of grass and shrub biomass using species-specific allometric equations (for shrubs only – see Table 6) based on height and cover. Specifically, the percentage coverage of each fuel class, as well as rockiness and soil, for each transect (Co; %) was calculated by dividing the number of intersections of the j-th fuel class (or rock or soil) by the total number of intersections along the transect (10 m \div 2 m = 5).

ATTRIBUTE	DATA TYPE	UNITS	OBLIGATION
INSTITUTE	CHAR	NA	mandatory
CHRONO_ID	CHAR	NA	mandatory
SITE_ID	CHAR	NA	mandatory
PLOT_ID	INTEGER	NA	mandatory
TRANSECT_ID	INTEGER	NA	mandatory
DISTANCE	INTEGER	NA	mandatory
ROCK_PRESENCE	BOOLEAN	NA	mandatory
SOIL_PRESENCE	BOOLEAN	NA	mandatory
LITTER_PRESENCE	BOOLEAN	NA	mandatory
LITTER_DEPTH	INTEGER	cm	mandatory
GRASS_PRESENCE	BOOLEAN	NA	mandatory
GRASS_DEPTH	INTEGER	cm	mandatory
SH_PRESENCE	BOOLEAN	NA	mandatory
SH_DEPTH	BOOLEAN	NA	mandatory
SH_SPECIES	CHAR	NA	mandatory
DATE	DATE (YYYY-MM-DD)	NA	mandatory

TRANSECT_ID – transect ID within the plot (from 1 to 3)

DISTANCE – distance from the origin (from 0 to 30, every 2 m; 15 sampling points in total)

ROCK PRESENCE – presence of rock (0 = no; 1 = yes)

SOIL PRESENCE – presence of bare soil (0 = no; 1 = yes)

LITTER_PRESENCE – presence of litter (0 = no; 1 = yes)

LITTER_DEPTH – depth of the litter (cm)

GRASS_PRESENCE – presence of grass (0 = no; 1 = yes)

GRASS_DEPTH – depth of the grass layer (cm)

SH_PRESENCE – presence of shrub (0 = no; 1 = yes)

SH_DEPTH – depth of the SH layer (cm)

SH SPECIES – dominant species of the SH layer





Figure 20. Sampling scheme for the different fuel categories: Above, the positioning of the three linear transects in an equilateral triangle. Below, an example of measuring the presence/absence and depth of fuel biomass relative to the ground in a coniferous forest.

Very fine woody debris and litter

Litter was collected from three square plots, each measuring 40×40 cm, enclosed by a metal frame and positioned at the centre of the three transects used for downed deadwood surveys



Figure 21). The litter collected included:

- **OL horizon:** Plant residues (primarily whole leaves, slightly altered or weakly fragmented) whose original shape remains clearly recognizable to the naked eye.
- OF horizon: Fragmented and partially decomposed plant tissues, still identifiable to the naked eye, mixed with a variable (but not predominant) amount of fine organic matter.
- 1-hour fuel (1h): Twigs and wood fragments with a diameter ranging from 0 to 0.6 cm.
- **10-hour fuel (10h):** Twigs and wood fragments with a diameter ranging from 0.6 to 2.5 cm.

The collected litter was placed in numbered plastic bags. Once returned to the laboratory, the bags were stored at 4°C for further analysis. In the lab, the contents of each bag were separated into the three fuel classes (OL and OF horizons, 1-hour and 10-hour fuel), and the fresh weight of each class was recorded (Pu; g). All samples were then dried in an oven at 90°C for 48 hours, after which the dry weight (Ps; g) of each sample—i.e., the oven-dried weight—was determined. The percentage moisture content on a dry-weight basis for each sample (U; %) was calculated as the difference between the wet and dry weights, divided by the dry weight. The average moisture content for each sampling area was derived as the mean of the moisture values from its three samples.



Figure 21. Litter and soil sampling scheme: red dots indicate sampling points (approximately midway along each transect). On the right is an example of litter sampling in a coniferous forest.

3.6. Soil survey

After litter collection, a soil sample was taken at each sampling point to a depth of 40 cm. A split-tube soil corer with a diameter of 53 mm and a length of 40 cm was used for this purpose (Figure 22).



Figure 22. Soil sampler.

The collected core was cut into its two main layers (the OH organic horizon and the mineral horizon) based on colour differences (Figure 23). On the sampling datasheet, the thickness of both the organic horizon and the mineral horizon (in cm) was recorded. Once in the laboratory, the samples were dried for bulk density determination and further analysis at the CHN Elemental Analyzer.

REWILD-FIRE - Deliverable 2.1



Figure 23. Separation of the soil horizons of the collected core

ATTRIBUTE	DATA TYPE	UNITS	OBLIGATION
Sampling area code	INTEGER	NA	mandatory
Sampling Point	INTEGER	NA	mandatory
Litter	BOOLEAN	NA	mandatory
Horizon	CHAR	NA	mandatory
Depth	INTEGER	cm	mandatory
Total fresh weight	INTEGER	g	mandatory
Stone weight	INTEGER	g	mandatory
Fresh weight soil < 2mm	INTEGER	g	mandatory
Dry weight soil < 2mm	INTEGER	g	mandatory
Core diameter	INTEGER	cm	mandatory
Volume	INTEGER	cm ³	mandatory
Bulk_density	INTEGER	g/cm ³	mandatory
Hole depth	INTEGER	cm	mandatory

Sampling area code – Sampling Area code (ZXn – YYYY)

Sampling point – number (1 to 3)

Litter – presence of litter (0 = no; 1 = yes)

Horizon – Type of horizon (O = Organic; M = Mineral)

Depth – depth of soil horizon (cm)

REWILD-FIRE - Deliverable 2.1

Total fresh weight - weight of sample (g - in lab)

Stone weight - weight of sample (g - in lab)

Fresh weight soil < 2 mm - weight of sample (g - in lab)

Dry weight soil < 2 mm - weight of sample (g - in lab)

Core diameter - diameter of corer (cm)

Volume - volume of sample horizon (cm³)

Bulk_density - of sample, calculated (g/cm³)

Hole depth - Total depth of the hole (cm)

4. Assessment of the aboveground carbon stock

4.1. Standing living trees

Biomass of living trees (B_{trees}; kg) was estimated using the R package *allodb* starting from the individual dendrometric data collected in the field at the plot level. This package contains a wide list of published allometric equations and functions proposed to compute aboveground biomass (Gonzalez-Akre et al., 2022). The data component of the package is based on 701 woody species identified at 24 large Global Earth Observatory (ForestGEO) plots representing a wide diversity of extratropical forests. The *allodb* package includes 570 allometric equations to estimate individual-tree biomass. The authors checked and combined the equations using a weighting function designed to ensure optimal equation selection over the full tree size range with smooth transitions across equations. If needed, the dataset of allometric equations can be customized with built-in functions that subset the original dataset and add new equations. Although equations were curated based on a limited set of forest communities and number of species, this resource is appropriate for portions of the global extra-tropics. Missing equations for the species surveyed in the field were retrieved from literature or local information, where possible.

To calculate the biomass of living trees using *allodb* (Figure 24), a table (i.e., dataframe *sensu* R) with DBH (cm), parsed species Latin names (genus and species names separately), and site(s) coordinates (reference system: WGS84) was needed. The species were then identified among the 701 woody species already embedded in the database of the package. In case no valid allometric equation was available for the species, the existence of an equation for the genus was checked. If none was available for the genus either, the most general equation at the family level was used. For example, there was no equation for *Salix caprea*, and hence an equation for the genus *Salix* was used. No equation for *Sorbus aucuparia* was present in the package and neither for the genus *Sorbus*; thus, a generic equation for the family *Rosaceae* was chosen to calculate the biomass.

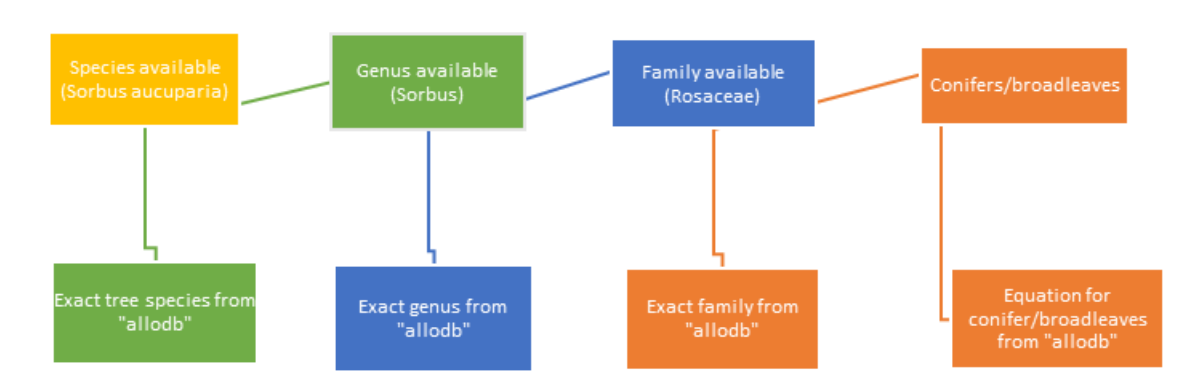


Figure 24. Workflow to associate the allometric equation to compute aboveground biomass of an individual tree knowing its species and DBH.

Total aboveground biomass at the site level was then calculated as the sum of all surveyed trees and expressed as tons per hectare (Mg ha⁻¹), considering the size of the plot on which the trees were surveyed.

4.2. Root biomass of standing living trees

The root biomass per hectare of standing trees at the plot or site level (B_{roots}; Mg ha⁻¹) was estimated using the following equation:

$$B_{roots} = RS \times B_{trees}$$

where RS is the root-to-shoot ratio reported by IPCC (2006) and B_{trees} is the total tree aboveground biomass (t ha⁻¹) (Table 3).

Table 3. Values of the root-to-shoot ratio (RS) according to IPCC (2006).

Aboveground biomass (AGB)	Root-to-shoot ratio (RS)
AGB < 75 t ha ⁻¹	0.43
75 t ha ⁻¹ ≤ AGB < 150 t ha ⁻¹	0.26
AGB ≥ 150 t ha ⁻¹	0.24

4.3. Deadwood biomass

Standing dead trees

For unbroken standing dead trees, biomass was estimated using the same procedure as in the case of living trees (i.e., *allodb* package; Gonzalez-Akre et al., 2025). A biomass reduction factor was then applied to correct the potential overestimation resulting from lower wood density in different decay stages. The reduction factors (RF) were calculated from the data by Bitunjac et al. (2023) for broadleaves and conifers according to the equation:

$$RF = \frac{\sigma_{decay}}{\sigma_{base}}$$

where σ_{decay} is the basic density of a specific decay class and σ_{base} is the basic density of living trees (0.596 and 0.468 g cm⁻³ for broadleaves and conifers, respectively; Bitunjac et al., 2023). The specific reduction factors for broadleaves and conifers by decay stage are reported in Table 4.

Table 4. Reduction factors for broadleaves and conifers by decay stage

Taxonomic group	Decay class	Reduction factor
	1	0.91
	2	0.76
Broadleaves	3	0.59
	4	0.42
	5	0.26
	1	0.80
	2	0.71
Conifers	3	0.58
	4	0.42
	5	0.34

Broken standing dead trees (snags)

The biomass of broken standing dead trees (B_{snag} ; kg), was quantified according to the equation:

$$B_{snag} = \frac{\pi}{4} \times \left(\frac{dbh}{100}\right)^2 \times h_{snag} \times FF \times \sigma_b$$

where h_{snag} is the height of the snag (m). FF is an average form factor (i.e., FF = 0.5) used to consider stem taper; σ_b is the basic density (kg m⁻³) of the deadwood for the specific decay class (see below).

Standing dead biomass (unbroken dead trees and broken snags) at the plot level was finally expressed per hectare, taking into account the size of the plot (Mg ha⁻¹).

Root biomass for the unbroken dead trees and broken snags was computed following the procedure adopted for standing living trees described above.

Coarse woody debris

The biomass of coarse woody debris (B_{CWD} ; kg), i.e. lying logs with a diameter >10 cm was quantified using the formula below, based on the equation of a truncated cone:

$$B_{CWD} = \frac{\pi}{4} \left(D_b^2 + D_t^2 + D_b D_t \right) \frac{l_{log}}{3} \times \sigma_b$$

where D_b and D_t are the diameters at the base and at the top of the lying deadwood (log)(all are expressed in m), respectively. I_{log} is the length of lying deadwood piece (m); σ_b is the basic density of lying deadwood decay class (see below). g

The total biomass of the coarse woody debris found in each plot was finally scaled to hectare taking into account the size of the plot (Mg ha⁻¹).

Fine woody debris

The biomass of fine woody debris (B_{CWD}; Mg ha⁻¹) was calculated according to the following equation (Harmon et al., 1996):

$$B_{FWD} = \frac{9.859}{8} \times \sum_{i=1}^{n} \frac{d_i^2}{L} \times \sigma_i$$

where d_i is the diameter of the piece of fine deadwood i (cm) intercepted by a linear transect in the field, σ_i is the basic density of the decay class (see below) and L is the length of the transect (m).

Stumps

The biomass of the stumps (kg) was determined according to the equation:

$$B_{stump} = \frac{\pi}{4} \times \left(\frac{d_{stump}}{100}\right)^2 \times h_{stump} \times \sigma_b$$

where d_{stump} and h_{stump} are the average diameter (cm) and average height (m) of the stump, respectively; σ_b is the basic density of the stump decay class (see below). The biomass of the stump's roots was determined according to the equation:

$$B_{root\ stump} = B_{stump\ as\ a\ tree} \times RS$$

where B_{stump_as_a_tree} is the biomass of a tree of DBH equal to the diameter of the stump calculated using the *allodb* R package and RS is the root-to-shoot ratio. Also in this case, all data were scaled to the hectare, considering the size of the plot.

Basic density of deadwood by decay stage

Standard basic density of deadwood by decay class reported in the literature for main European tree species were used to calculate deadwood biomass. In particular, density values provided by Bitunjac et al. (2023) for five broadleaf (*Quercus, Carpinus, Alnus, Fraxinus, Fagus*) and three conifer genera (*Abies, Picea, Pinus*) were considered. If the species of the deadwood piece was not included in the dataset or was not identified, the basic density of broader categories (i.e., broadleaves and conifers) was applied (Bitunjac et al. 2023; Table 5).

Table 5. Dead wood basic density (DWBD) by decay classes retrieved from Bitunjac et al. (2023) and obtained using pooled data from the literature survey and data from an experimental study conducted by the authors, for tree genera separately, and combined into Broadleaves and Conifers groups.

Genus	Decay class	Dead wood basic density (g cm ⁻³)
	1	0.422
	2	0.359
Alnus	3	0.286
	4	0.197
	5	0.120
	1	0.392
	2	0.428
Carpinus	3	0.339
·	4	0.211
	5	0.140
	1	0.555
	2	0.388
Fagus	3	0.264
_	4	0.248
	5	0.220
	1	0.527
	2	0.431
Fraxinus	3	0.392
	4	0.265
	5	0.151
	1	0.617
	2	0.519
Quercus	3	0.397
	4	0.299
	5	0.196

	1	0.343
	2	0.305
Abies	3	0.247
	4	0.174
	5	0.149
	1	0.381
	2	0.340
Picea	3	0.270
	4	0.190
	5	0.157
	1	0.379
	2	0.334
Pinus	3	0.277
	4	0.214
	5	0.165
	1	0.542
	2	0.450
Broadleaves	3	0.349
	4	0.251
	5	0.153
	1	0.375
	2	0.334
Conifers	3	0.271
	4	0.198
	5	0.160

Grass and shrub biomass

The biomass per hectare of the herbaceous layer (B_{grass}; Mg ha⁻¹) and shrubs (B_{shrub}; Mg ha⁻¹) were calculated using the allometric equations in Table 6.

Table 6. Allometric equations for calculating the biomass per hectare of the herbaceous and shrub layer. C = coverage expressed in %; H = depth in cm.

	Grass						
Height	Equations	Source					
< 20 cm	= (3.003*LN(Co)+1.207)/10	Charles B. Halpern					
		and Eric A. Millet,					
		1996					
> 20 cm	= Co/100 * (-0.0038 * H^2 + 0.25 * H)	Bovio e Ascoli, 2013					
> 40 cm	= 0.1778 *H * Co/100 - 0.052	Mou G, 2015					
	Shrubs						
Species	Equations	Source					
Ferns	= 0.0010 * H^1.6430 *	Vega et al., 2022					
	ARCSEN(RADQ(Co/100)))^0.3705						
Erica	=0.0294*H^0.9054*(ARCSEN(RADQ(Co)))^0.5545	Vega et al., 2022					
Ulex	= 0.1111*H^0.7087*(ARCSEN(RADQ(Co)))^0.2868	Vega et al., 2022					
Calluna	= 0.09*(Co/100)*(10000*(H/100)^1.06)	Gonzalez et al. 2013					

Rubus	= (0.2508*(Co)^0.7885)/100)	Smith and Brand, 1983
Caminta	- C-/400 * (007 · F 00*LI)/400	
Genista	= Co/100 * (937+5.99*H)/100	Castagneri et al., 2013
Myrtillus	= (0.1496*Co) ^{\lambda0.934})/100	Smith and Brand,
		1983
Juniperus	= 0.10*(Co/100) ^{2*} ((H/2)*0.405)	Riccardi et al., 2007

For those species or genera that were not included in Table 6, total biomass (B_{total} in t ha⁻¹) was estimated using the general equations for macro-phanerophytes by De Cáceres et al. (2019):

$$\begin{split} CA_m &= 5.8458 \times H_m^{1.4944} & [cm^{-2}] \\ B_{total,m} &= 0.7856 \times V_{total}^{0.8101} = 0.7856 \times (\frac{H_m}{100} \times \frac{CA_m}{10000})^{0.8101} & [kg \ individual^{-1}] \\ N &= \frac{C}{100} \times \frac{10000}{CA_m} = \frac{C \times 100}{CA_m} & [plants \ m^{-2}] \\ B_{total} &= \frac{N \times B_{total,m}}{1000} \times 10000 & [t \ ha^{-1}] \end{split}$$

where CA_m is the estimated projected crown area of an average individual (cm²) derived from the measured mean height (H_m in cm); B_{total,m} is the biomass of an average individual (kg individual⁻¹); V_{total} is the apparent shrub volume (m³); N is estimated shrub density (individuals m⁻²) and C is the measured cover (in %).

Grass root biomass was calculated using a root-to-shoot ratio of 4, as suggested by IPCC (2006) for boreal (Dry & Wet), cold temperate wet and warm temperate wet grasslands. Shrub root biomass was calculated using the same approach as for the roots of standing living trees.

Carbon content

Living biomass: the conversion from biomass to C stock (MgC ha⁻¹) was obtained using an average C content of 0.47 (IPCC 2006).

Dead biomass: the conversion of biomass into C stock was carried out considering a carbon content (%) retrieved from the literature. According to Bitunjac et al. (2023), the C fraction remains largely constant across decay stages, and thus for this study an average of 0.475 for the broadleaves and 0.505 for conifers is being used (Bitunjac et al. 2023).

4.4. Very fine woody debris and litter

The biomass per hectare (B; t ha⁻¹) of very fine woody debris and litter was estimated for the 1-hour and 10-hour fuel classes using the following equation:

$$B = P_u \times (1 - U_{AdS}) \times \frac{1}{1000000} \times \frac{10000}{0.40 \times 0.40}$$

For the conversion to C stock, a standard carbon content of 50% was used for wood. For the OL and OF horizons, after homogenizing each sample, a subsample was used to determine the carbon content via CHN analysis.

5. Assessment of soil carbon stock

To determine the bulk density of the soil (σ_{bulk} ; kg m⁻³), the following steps were carried out:

- 1. Weigh and record the fresh weight of the entire sample (Pftot; g);
- 2. Sieve the soil to 2 mm and measure the fresh weight of the coarse fraction (Pfsc; g);
- 3. Take and weigh a subsample of the fine earth fraction (Pf_{TF}; g);
- 4. Dry the fine earth subsample at 70°C for 48 hours;
- 5. Determine the oven-dry weight of the subsample (Ps_{TF}; g).
- 6. Calculate the moisture content of the subsample: $U = (Pf_{TF} PS_{TF})/PS_{TF}$

The bulk density was then calculated as:

$$\sigma_{bulk} = \frac{Ff_{tot} - Pf_{sc}}{\frac{1+U}{S \times h}} \times 1000$$

where S is the cross-sectional area of the soil corer (cm²), and h is the depth of the horizon considered (cm). From the fine earth subsample, a portion of soil was taken and pulverized using a ball mill. The sample was then prepared for CHN elemental analysis, following a treatment with HCl to remove any carbonates present (Nieuwenhuize et al., 1994). Each CHN analysis was performed in duplicate. The C stock in the considered soil horizon (C_soil; tC ha⁻¹) was calculated using the following equation:

$$C_{suolo} = \frac{h}{100} \times 10000 \times \frac{\sigma_{bulk}}{1000} \times \%C$$

where:

- **h** is the depth of the considered horizon (organic or mineral) in cm,
- σ_bulk is the bulk density of the soil in kg m⁻³,
- %C is the carbon concentration measured via CHN analysis

6. Main results and discussion

6.1. Description of the dataset

The dataset on aboveground data, which includes dendrometric data, measurements of coarse and fine woody debris, and fuel, consists of 12 replicated chronosequences encompassing a total of 197 sites. These comprise 8 replicated chronosequences from afforestation (125 sites) and 4 from proforestation (72 sites). In total, dendrometric data were collected for 7,208 trees — 4,857 trees from afforestation sites and 2,351 from proforestation sites. The full list of chronosequences included in this dataset is provided in Table 7.

Table 7. List of the chronosequences constituting the dataset of this deliverable. Chrono id = id of the chronosequence; land use = land use before the secondary succession afforestation took place (G=grassland; C=cropland) or we are in a proforestation site (P).

N	Ecoregion	Sub-ecoregion	Region	Chrono id	Age Range	N. of sites	Land use
1		1A2a	Friuli Venezia Giulia (Taipana)	UNIUD_1	0–75	20	G
2		IAZa	Friuli Venezia Giulia (Faedis)	UNIUD_5	0–75	15	С
3		1A2b	Friuli Venezia Giulia (Ampezzo)	UNIUD_6	0–75	15	G
4		IAZD	Friuli Venezia Giulia (Ampezzo)	UNIUD_7	0–75	15	С
5		1A1b	Piemonte	UNITO_1	0–75	15	G
6	Alpine		Piemonte	UNITO_2	0–75	15	С
7		1A2c	Lombardia	CA1 – 3	0–75	15	G
8		TAZC	Lombardia	CP1 – 3	0–75	15	С
9		1A2a	Friuli Venezia Giulia (Cansiglio)	AF 1 – 9	0–100	27	Р
10		1A2b	Friuli Venezia Giulia (Val Alba)	BF 1 – 9	0–100	27	Р
11		1A1b	Piemonte	CF 1 – 3	10–60	9	Р
12		1A2c	Lombardia	DF 1 – 3	10–74	9	Р
					TOTAL	197	-

6.2. Afforestation

Aboveground C stocks

The average number of living trees per hectare across all afforestation sites was 1298 ± 144 (Table 8). Tree mortality across all sites and ecoregions (number of dead trees on total number of trees) increased linearly with time since abandonment (TSA), reaching a maximum of $23 \pm 5\%$ at 34 years, and then decreased to $16 \pm 4\%$ at 75 years (y = -1E-04x² + 0.0094x + 0.0089; R²=0.96). Mean tree diameter showed a consistent and significant increase over TSA.

Total aboveground C stocks increased linearly with TSA in all ecoregions and for both initial land uses, i.e. cropland and grassland (

Figure 25). All linear trends for each combination of ecoregion and land use showed high R² values and statistically significant p-values, indicating a good fit of the data. However, comparison of the model slopes using a Linear Mixed Model (LMM) revealed no clear

differences among groups, suggesting that the trends were generally consistent across both ecoregions and land uses. The only exception was ecoregion 1A2c, which showed the steepest increase in aboveground C stocks over time (p-value = 0.003), with an additional rate of 1.10 tC ha⁻¹ year⁻¹ above the baseline rate of 2.10 tC ha⁻¹ year⁻¹. Ecoregions 1A2b and 1A1b showed no significant differences from the reference ecoregion 1A2a in their accumulation rates (p-values = 0.671 and 0.288, respectively). Based on these results, we recomputed the regressions between total aboveground C stocks (including roots) and TSA, grouping the data by ecoregion only (Figure 26). The rate of increase in aboveground C stocks, including roots, ranged from 1.71 to 3.20 tC ha⁻¹ year⁻¹ in ecoregion 1A1b and 1A2c, respectively.

Although studies examining secondary succession on abandoned agricultural land and reporting aboveground C stock dynamics in relation TSA are limited, our results are consistent with the previous findings. In fact, a recent literature search on this topic covering studies published over the past 30 years (1994–2024) revealed that only a limited number of investigations report data on aboveground biomass or C accumulation during secondary succession on former agricultural land (Alberti et al., 2024). Moreover, many of these studies rely on chronosequences from artificially reforested sites, rather than examining patterns of natural vegetation recolonization. The majority of studies were conducted in Italy (7) and Poland (3), with a higher density in the Continental and Alpine ecoregions. A total of four studies focused specifically on the Alpine region (Thuille and Schulze, 2006; Alberti et al., 2008; Guidi et al., 2014; Risch et al., 2008).

Looking at these studies, Thuille and Schulze (2006) reported an increase in stem biomass carbon during spruce (Picea abies) secondary succession, reaching up to 250-400 tC ha⁻¹ in the oldest successional stands (93–112 years old). This corresponds to a mean annual C uptake of approximately 2.69 to 3.57 tC ha⁻¹ year⁻¹. In contrast, Guidi et al. (2014), although not specifying the exact age of the stands studied, found lower aboveground C stocks in standing trees, measuring approximately 100 tC ha⁻¹ in the oldest spruce-dominated secondary forests. Risch et al. (2008) reported aboveground C stocks ranging from 0.1 tC ha⁻¹ in short-grass pastures to 166 tC ha⁻¹ in mixed conifer and stone pine–larch forests in Switzerland. Using a mountain pine stand age of 156 years, this corresponds to an annual mean uptake of 1.06 tC ha⁻¹ year⁻¹. Alberti et al. (2008) for ash and maple mixed stands in the Eastern Italian Prealps reported a mean C uptake of 1.69 tC ha⁻¹ year⁻¹.

Table 8. Major dendrometric characteristics by original land use, eco-region and time since abandonment. G = basal area. Mean \pm standard error.

ORIGINAL LAND USE	ECOREGION	CLASS AGE	Tree density alive (N ha ⁻¹)	Tree density dead (N ha ⁻¹)	G alive (m² ha-¹)	G dead (m² ha ⁻¹)	Mean diameter alive (cm)
		0	0 ± 0	0 ± 0	0 ± 0	0 ± 0	0 ± 0
		13	2923 ± 681	707 ± 247	22.93 ± 4.23	2.68 ± 0.94	10 ± 1
	1A2a	34	2171 ± 1039	546 ± 280	32.86 ± 9.98	3.28 ± 1.26	16 ± 3
		57	1398 ± 352	357 ± 338	39.22 ± 3.53	2.23 ± 1.32	20 ± 3
		75	779 ± 120	255 ± 52	46.62 ± 3.83	8.92 ± 3.45	28 ± 1
		0	0 ± 0	0 ± 0	0 ± 0	0 ± 0	0 ± 0
		13	1858 ± 715	31 ± 17	21.78 ± 5.38	0.69 ± 0.47	13 ± 1
	1A2b	34	1816 ± 867	527 ± 243	26.42 ± 5.02	4.48 ± 0.5	16 ± 3
		57	1862 ± 938	63 ± 35	37.17 ± 3.85	1.91 ± 0.11	22 ± 7
Cropland		75	1047 ± 449	98 ± 70	45.4 ± 9.35	2.23 ± 1.27	27 ± 6
Cropiand		0	0 ± 0	0 ± 0	0 ± 0	0 ± 0	0 ± 0
		13	1146 ± 325	249 ± 33	21.62 ± 5.34	1.48 ± 0.47	16 ± 0
	1A2c	34	2316 ± 1027	947 ± 748	27.94 ± 6.24	3.04 ± 2.38	13 ± 1
		57	1763 ± 753	767 ± 245	48.97 ± 4.82	3.75 ± 1.54	25 ± 9
		75	1947 ± 507	255 ± 209	54.66 ± 5.5	4.26 ± 2.02	21 ± 4
		0	38 ± 38	6 ± 6	0.63 ± 0.63	0.44 ± 0.44	5 ± 5
	1A1b	13	651 ± 197	38 ± 19	11.9 ± 0.46	0.38 ± 0.15	17 ± 3
		34	1079 ± 263	587 ± 445	20.38 ± 0.58	3.52 ± 1.75	17 ± 3
		57	1178 ± 583	401 ± 299	21.59 ± 2.48	2.26 ± 0.02	18 ± 3
		75	1275 ± 356	650 ± 224	33.28 ± 4.28	3.66 ± 1.54	19 ± 3
	1A2a	0	0 ± 0	0 ± 0	0 ± 0	0 ± 0	0 ± 0
		13	2585 ± 817	210 ± 115	22.08 ± 4.19	2.16 ± 1.07	11 ± 1
		34	1732 ± 647	985 ± 614	23.62 ± 0.71	4.74 ± 0.87	15 ± 3
		57	2499 ± 778	317 ± 125	31.4 ± 3.95	3.36 ± 0.96	14 ± 2
		75	2119 ± 709	198 ± 90	40.52 ± 5.02	5.13 ± 3.57	19 ± 5
		0	0 ± 0	0 ± 0	0 ± 0	0 ± 0	0 ± 0
		13	3080 ± 1250	13 ± 13	18.64 ± 4.63	1.53 ± 1.53	9 ± 1
	1A2b	34	3178 ± 647	25 ± 17	31.62 ± 3.96	0.96 ± 0.62	12 ± 2
		57	1486 ± 455	255 ± 71	34.1 ± 9.98	8.63 ± 1.41	17 ± 2
Grassland		75	1123 ± 466	88 ± 31	39.9 ± 5.86	3 ± 1.21	23 ± 3
Grassianu		0	0 ± 0	0 ± 0	0 ± 0	0 ± 0	0 ± 0
		13	1720 ± 493	0 ± 0	21.3 ± 5.89	0 ± 0	13 ± 3
	1A2c	34	769 ± 261	303 ± 275	55.29 ± 12.71	4.1 ± 2.05	31 ± 2
		57	596 ± 44	177 ± 70	73.41 ± 2.98	3.52 ± 1.48	40 ± 2
		75	985 ± 356	38 ± 22	58.37 ± 2.47	1.91 ± 1.62	30 ± 5
		0	0 ± 0	0 ± 0	0 ± 0	0 ± 0	0 ± 0
		13	912 ± 437	567 ± 205	11.91 ± 3.72	3.3 ± 2.28	14 ± 2
	1A1b	34	1795 ± 555	82 ± 72	28.86 ± 2.23	1.37 ± 0.89	15 ± 2
		57	946 ± 266	356 ± 180	27.13 ± 4.63	2.66 ± 1.22	20 ± 1
		75	1134 ± 303	214 ± 51	37.95 ± 8.57	2.05 ± 0.49	22 ± 4

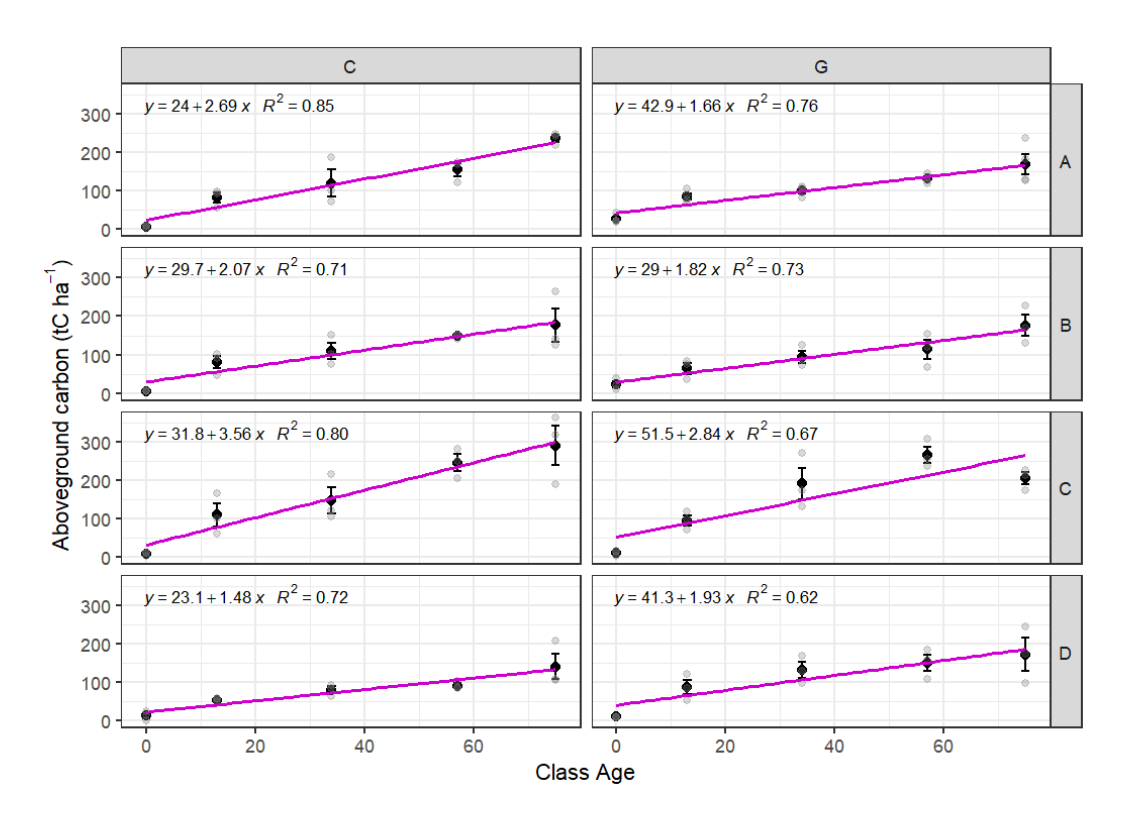


Figure 25. Total aboveground carbon stock including roots (tC ha^{-1}) as a function of time since abandonment (Class Age) by initial land use (C = cropland; G = grassland) and ecoregion (A =1A2a; B = 1A2b; C = 1A2c; D = 1A1b). Vertical bars represent standard errors.

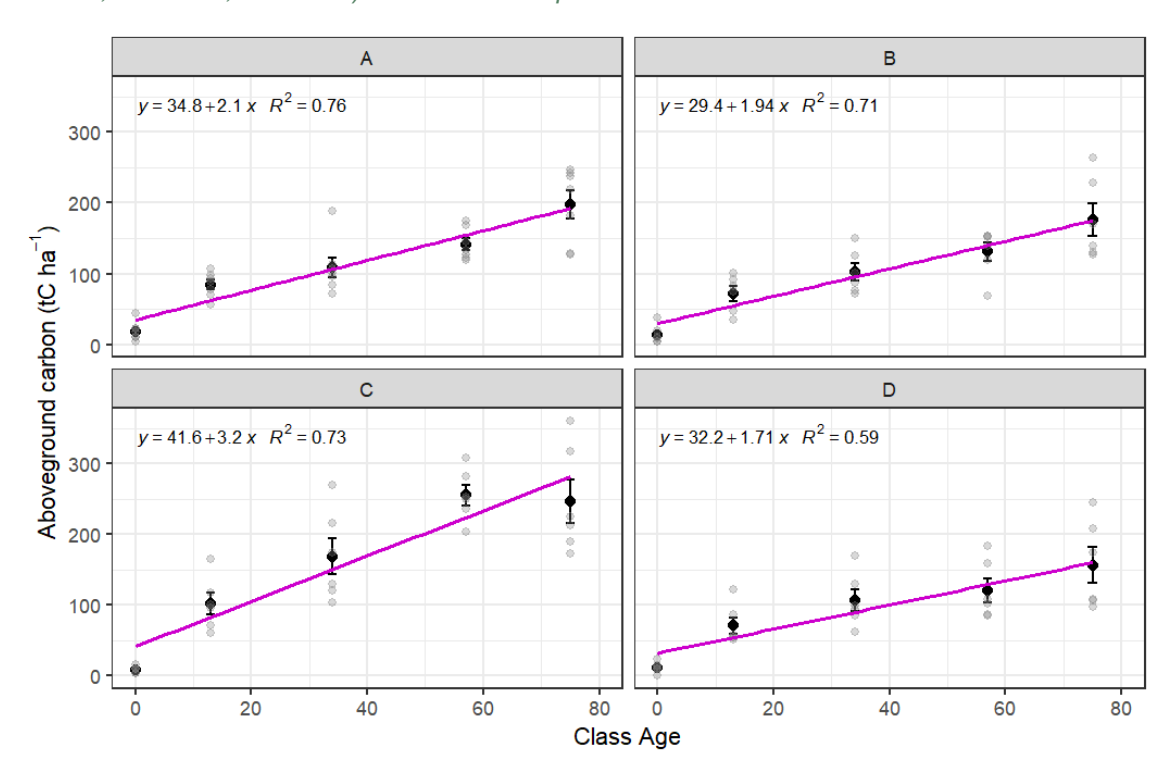


Figure 26. Total aboveground carbon stock including roots (tC ha^{-1}) as a function of time since abandonment grouped by ecoregion (A =1A2a; B = 1A2b; C = 1A2c; D = 1A1b). Vertical bars represent standard errors.

Soil C stocks

A linear mixed-effects model (LMM) was used to assess changes in total soil C in relation to TSA, ecological region, and their interaction. The model included random intercepts for each chronosequence and nested plot to account for spatial structure in the data. Parameter estimates were obtained using Restricted Maximum Likelihood (REML). The model revealed significant effects of ecological region, TSA, and their interaction on total soil C, while also accounting for land use before abandonment and random variation across sites.

Overall, total soil C increased significantly with TSA (+0.19 tC ha⁻¹ year⁻¹, p = 0.043,

Table 9), indicating a positive relationship between TSA and soil C accumulation. This coefficient corresponds to the baseline accumulation rate in ecoregion 1A2a, the reference level in the model. However, this effect varied significantly across ecoregions. Compared to ecoregion 1A2a, ecoregions 1A2b and 1A2c were associated with higher soil C stocks (+14.09 and +11.76 tC ha⁻¹, respectively), though these differences were only marginally significant (p = 0.107 and p = 0.177). In contrast, ecoregion 1A1b showed a significant lower total soil C stock (-19.70 tC ha⁻¹, p = 0.027), suggesting region-specific environmental constraints. Importantly, the interaction terms indicated that the rate of soi C accumulation with TSA was significantly moderated by ecoregion. In ecoregion 1A2b and 1A2c, the interaction was not statistically significant (p = 0.124 and p = 0.498), corresponding to a net rate of -0.01 tC ha⁻¹ year⁻¹ and +0.10 tC ha⁻¹ year⁻¹, respectively. In contrast, ecoregion 1A1b showed a significant negative interaction effect (-0.13 tC ha⁻¹ year⁻¹, p = 0.019), indicating no appreciable gain in soil C over time in this region, and potentially even a loss. Land use before abandonment had a positive but non-significant effect on soil C stock (+7.21 tC ha⁻¹, p = 0.178), indicating a possible trend toward higher overall soil C stocks under grasslands than under croplands, though further evidence is required.

Table 9. Results of the linear mixed-effects model (LMM) evaluating total soil C stocks (tC ha⁻¹) as a function of time since abandonment (TSA), ecoregion, previous land use, and their interactions. The model includes random intercepts for chronosequences and nested sampling plots to account for spatial structure. Estimates are based on REML; degrees of freedom were approximated using Satterthwaite's method. Reference levels: land use = cropland; ecoregion = 1A2a. Random effects: standard deviation of random intercepts = 11.14 tC ha⁻¹ (chronosequence), 11.42tC ha⁻¹ (nested plot); residual SD = 15.13tC ha⁻¹. Significance codes: *** p < 0.001; ** p < 0.01; * p < 0.05; † p < 0.10.

Fixed Effects	Estimate	Std. Error	Df	t value	p-value	Significance
Intercept	53.66	6.52	33.82	8.22	<0.001	***
TSA cropland	0.19	0.09	95.71	2.05	0.0429	*
Ecoregion 1A2b	14.09	8.55	38.95	1.65	0.1074	
Ecoregion 1A2c	11.76	8.55	38.95	1.38	0.1770	
Ecoregion 1A1b	-19.70	8.55	38.95	-2.30	0.0267	*
Grassland land use	7.21	5.16	19.99	1.40	0.1780	
TSA: Ecoregion 1A2b	-0.20	0.13	95.35	-1.55	0.1244	
TSA : Ecoregion 1A2c	-0.09	0.13	95.35	-0.68	0.4978	
TSA: Ecoregion 1A1b	-0.32	0.13	95.35	-2.39	0.0187	*

Random intercepts for chronosequence nested plot accounted for substantial variability in soil C content (variance = 124.0 and 130.4, respectively), confirming the importance of spatial structure in the data. Residual variance remained high (228.9), reflecting within-plot variability not explained by the fixed effects. The scaled residuals were approximately symmetric and

centered, although a few outliers were observed (min = -2.85; max = 4.67), indicating acceptable model performance (Figure 27).

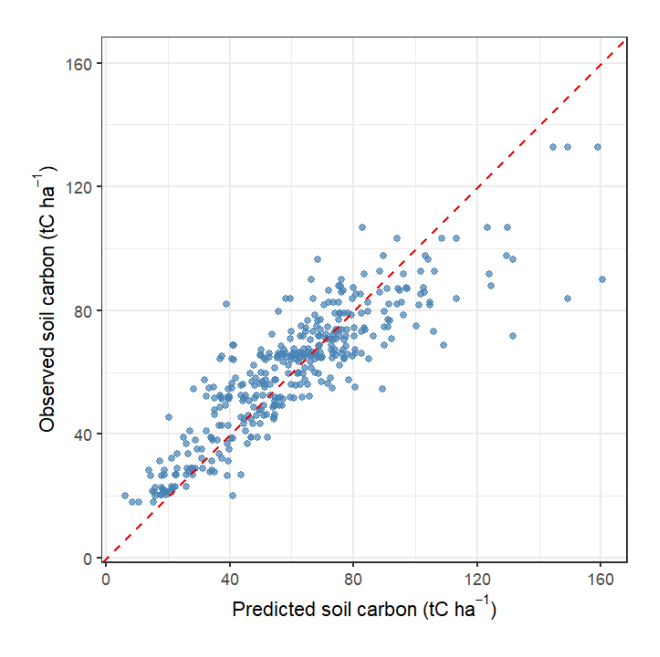


Figure 27. Comparison between predicted and observed soil carbon stocks.

Our results confirm that previous history and management is among the most decisive factors influencing the trend of soil organic carbon (SOC) change. Similar to what was reported by Guo and Gifford (2002), Nezhad et al. (submitted) also found a significant interaction between prior land use and ecoregion in shaping the relationship between SOC stocks and TSA. Their meta-analysis, which compiled data from 36 studies on passive reforestation following the cessation of agriculture, included 267 distinct mean relative SOC change (RSC) values covering various post-abandonment intervals. They observed that soil C stocks increased significantly over time when croplands were abandoned and subsequently colonized by broadleaf or mixed forests, with average annual increases of 0.19% and 0.33%, respectively, relative to active croplands. This can be attributed to the end of soil disturbance caused by plowing, which enhances microbial activity and C loss through aeration. The cessation of agricultural practices, combined with higher organic inputs from forest litter, supports C accumulation in the soil. The greater SOC gains observed in areas transitioning to mixed forests compared to those regenerating as pure broadleaf or conifer stands likely result from differences in litter quantity and quality, root architecture, and biomass productivity. Slower SOC accumulation in coniferous forests is probably due to their production of more resistant litter materials, such as pine needles, which decompose slowly (Prescott, 2002; Vesterdal et al., 2013). Our findings are also consistent with previous research by Laganière et al. (2010) and Paul et al. (2002), who also reported that reforesting croplands with mixed species enhances SOC accumulation. This effect is likely driven by increased biomass inputs, more diverse and deeper root systems, and enhanced microbial activity, all of which favour the formation of stable soil organic matter.

By contrast, grasslands abandoned after agricultural use did not exhibit clear trends of SOC gain. In many cases, soil C stocks remained stable or even declined slightly during the early stages of abandonment (

Table 9), a result in accordance with Nezhad et al. (submitted), suggesting that secondary succession on abandoned grasslands contributes little to SOC sequestration in the short term. Jackson et al. (2002) noted a negative correlation between precipitation levels and SOC changes in grasslands invaded by woody species. In humid environments, productive grasslands tend to channel more carbon into belowground biomass and often maintain higher SOC levels than regenerating forests.

Total ecosystem C stocks

Analysis of total ecosystem C stocks (tC ha⁻¹) in relation to TSA revealed significant linear trends across different land uses and ecoregions (Figure 28). The mixed-effects model identified a significant effect of TSA (stand age class; p < 0.001), with baseline C stocks estimated at 94.1 tC ha⁻¹ in the reference ecoregion 1A2a (labelled A in the figure). Carbon accumulation rates varied among ecoregions (Figure 29 and

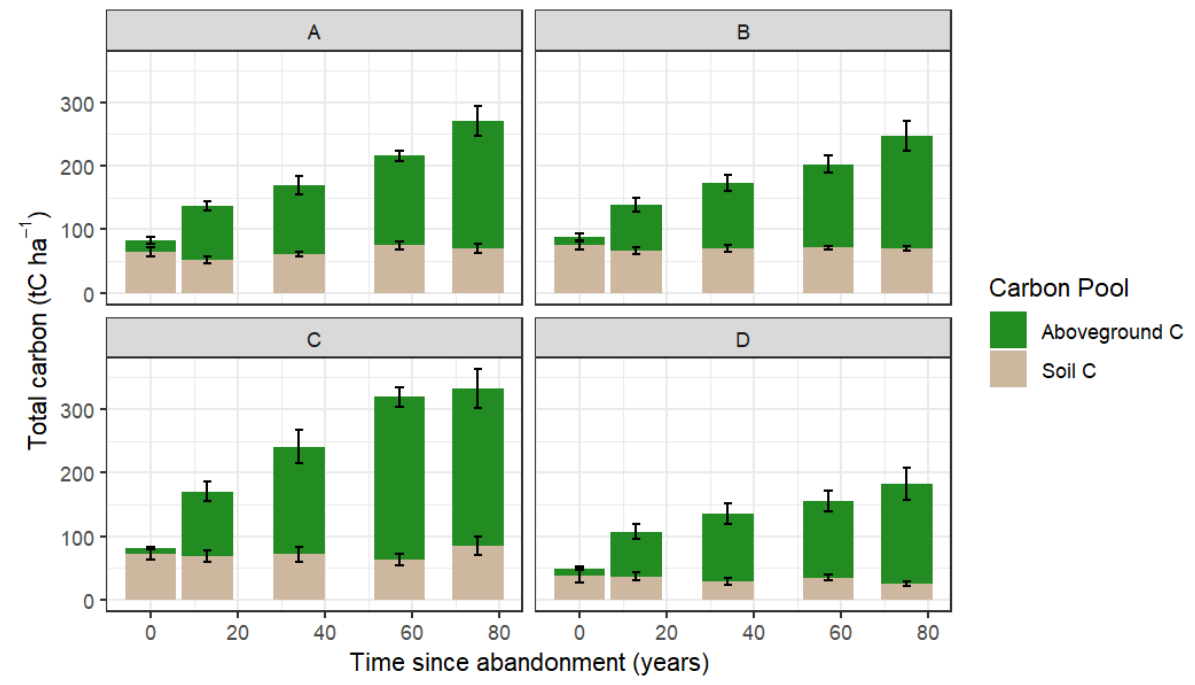


Figure 30). In ecoregion 1A2a, the estimated accumulation rate was 2.31 tC ha⁻¹ year⁻¹. Ecoregion 1A2b had a slightly lower, but statistically non-significant, rate of 1.93 tC ha⁻¹ year⁻¹ (p = 0.336). In contrast, ecoregion 1A2c exhibited a significantly higher rate of 3.30 tC ha⁻¹ year⁻¹ (p = 0.010), while ecoregion 1A1b showed a marginally lower rate of 1.58 tC ha⁻¹ year⁻¹ (p = 0.062). These findings indicate that inter-ecoregion differences are primarily driven by variation in C accumulation rates rather than initial carbon stock levels. Notably, the accumulation rate in ecoregion 1A2a (2.30 tC ha⁻¹ year⁻¹) is higher than some previous estimates for the Eastern Prealps (Alberti et al. 2008).

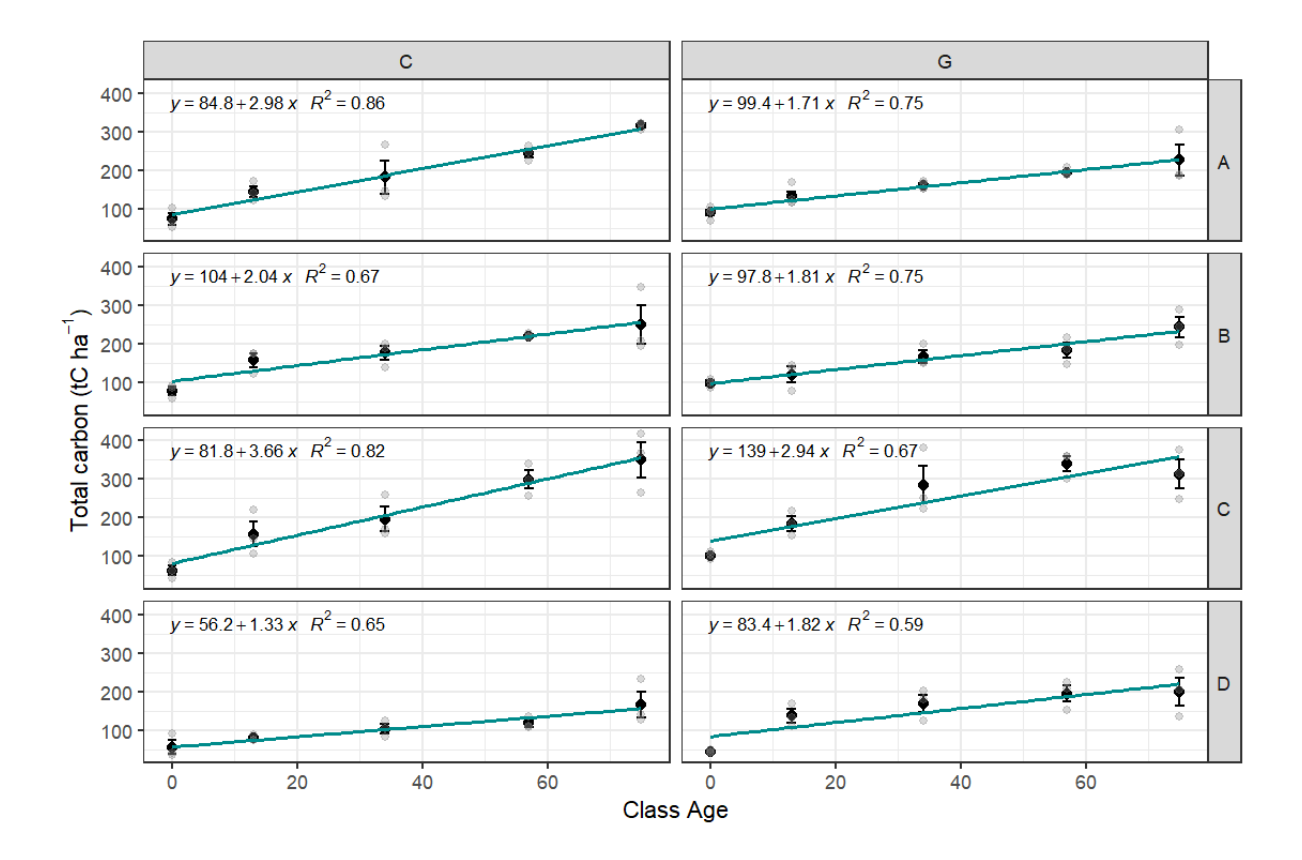


Figure 28. Total ecosystem carbon stock (aboveground + soil; tC ha⁻¹) as a function of time since abandonment, shown by initial land use (C = cropland; G = grassland) and ecoregion (A = 1A2a; B = 1A2b; C = 1A2c; D = 1A1b). Error bars indicate standard errors.

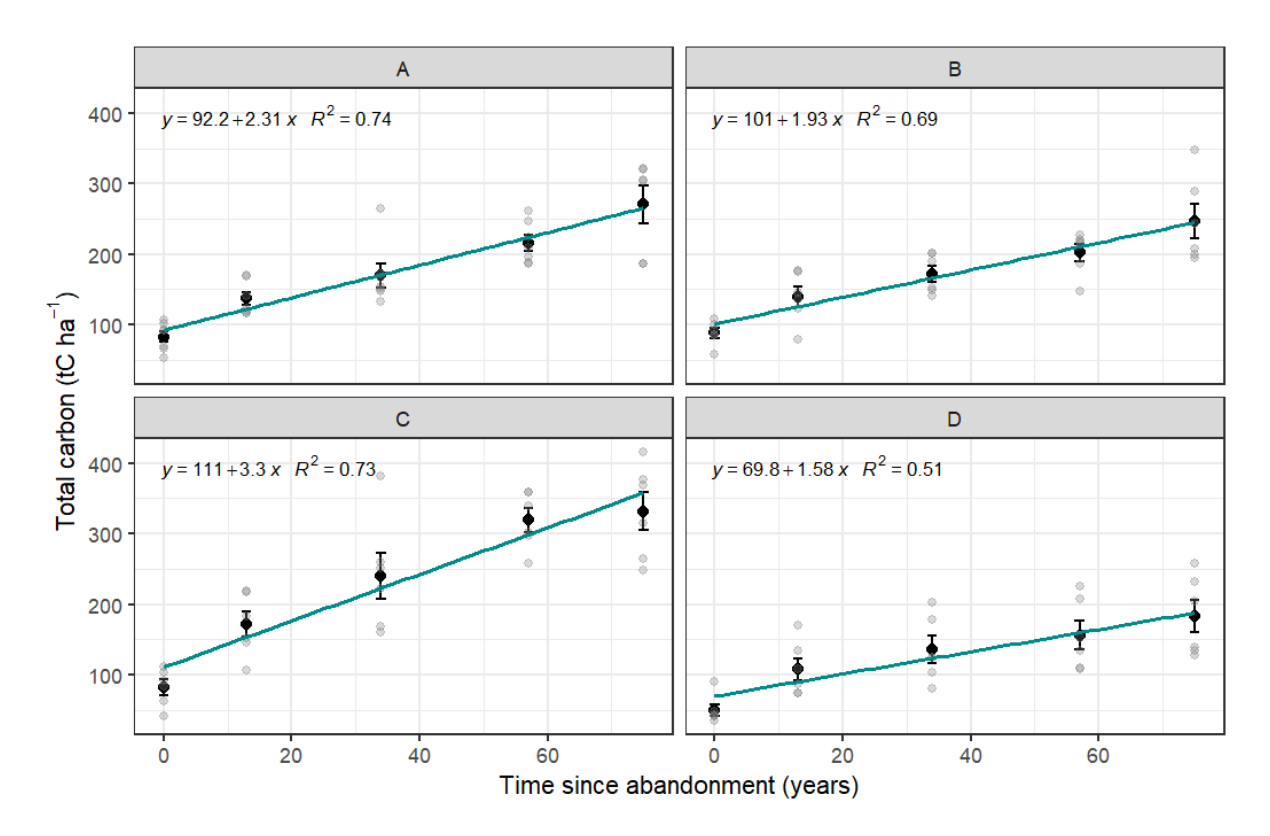


Figure 29. Total ecosystem carbon stock (aboveground + soil; tC ha⁻¹) as a function of time since abandonment, by ecoregion (A = 1A2a; B = 1A2b; C = 1A2c; D = 1A1b). Vertical bars represent standard errors.

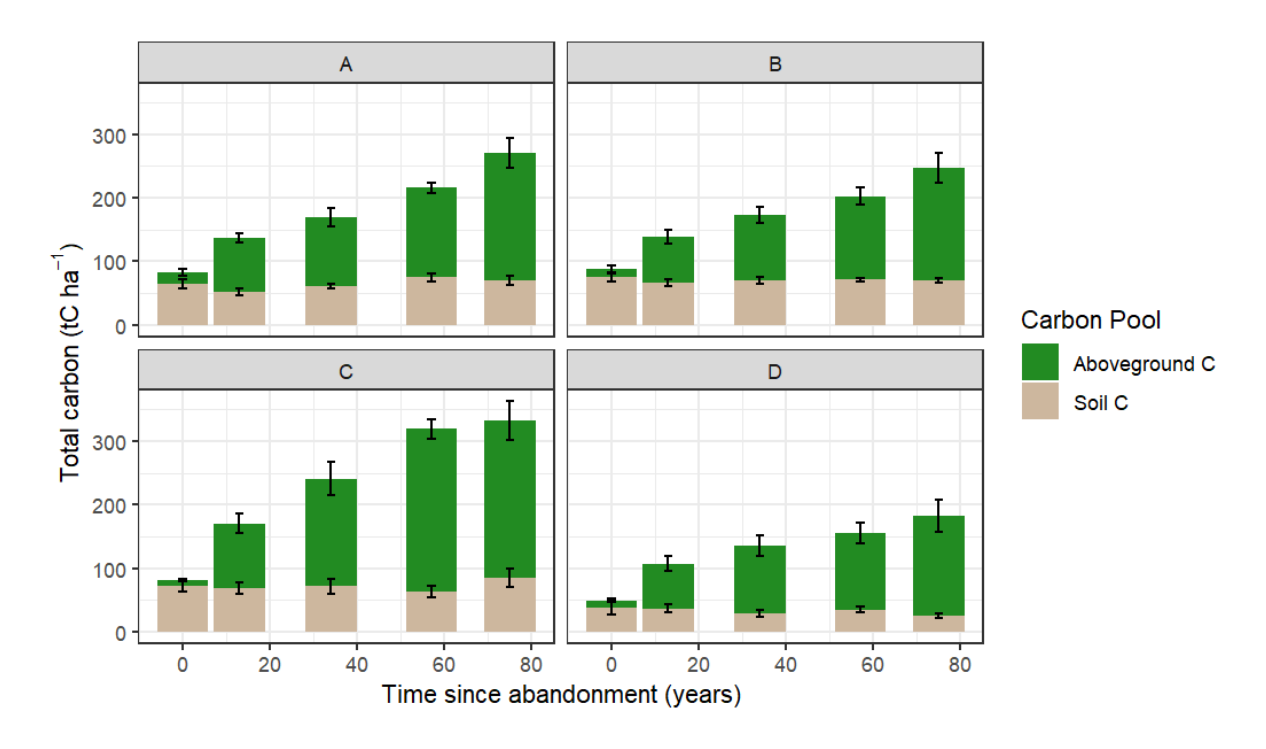


Figure 30. Partitioning of total ecosystem carbon stock (tC ha^{-1}) between aboveground component and soil as a function of time since abandonment, grouped by ecoregion (A = 1A2a; B = 1A2b; C = 1A2c; D = 1A1b). Error bars indicate standard errors.

6.3. Proforestation

Aboveground C stocks

The average number of trees per hectare did not significantly change between managed (MF) and abandoned forests (NM = not managed; and OG = old-growth) (Table 10) even though a slight increase in average diameter and basal area was detected (MF = 43.36 m² ha⁻¹; NM and OG: 50.84 m² ha⁻¹). A shift in the diameter distribution curves was also observed (Figure 31): over TSA, the curves gradually moved to the right, indicating larger diameters. Additionally, the number of standing dead trees and snags increased progressively with time.

Total aboveground C stocks — including living biomass in trees, shrubs, and grasses (and their roots), as well as dead biomass in standing trees, and coarse and fine woody debris — increased over time following the cessation of forest management (Figure 32). This upward trend was particularly pronounced in ecoregions 1A2b and 1A1b, where proforestation took place in former coppice stands that had been converted to high forests prior to abandonment. In contrast, the ecoregions 1A2a and 1A2c exhibited a delayed increase in total C stocks, with notable accumulation becoming evident only after approximately 60 years post-abandonment (OG stage); in these areas, high forests were present from the outset. Across all ecoregions, the proportion of C stored in dead biomass compartments — standing dead trees, snags, and lying woody debris — increased over time, likely driven by intensified competition among trees leading to natural mortality (Figure 33).

Table 10. Major dendrometric characteristics by eco-region, forest type and time since abandonment (TSA: MF = managed forests; NM = not-managed; OG = old-growth). Mean \pm standard error.

Ecoregion	TSA	European forest type	Tree density (N ha ⁻¹)	Basal area (m² ha ⁻¹)	Mean diameter (cm)
	MF		501 ± 54	57.14 ± 4.67	39 ± 2
1A2a	NM	7.2 Central European montane beech forest	355 ± 52	50.89 ± 5.23	44 ± 2
	OG		600 ± 119	76.28 ± 4.54	44 ± 4
	MF	7.2 Central European montane beech forest	483 ± 32	41.95 ± 1.47	33 ± 1
1A2b	NM		836 ± 151	44.79 ± 2.39	28 ± 2
	OG		1044 ± 96	58.73 ± 2.74	27 ± 1
	MF	6.3.2 Subalaina and mountainaus sarues and	1281 ± 178	53.48 ± 9.68	23 ± 1
1A2c	NM	6.3.2 Subalpine and mountainous spruce and mountainous mixed spruce-silver fir forest	585 ± 57	45.22 ± 3.85	31 ± 2
	OG		794 ± 173	55.03 ± 5.85	31 ± 4
	MF	6.7.1 South western European mountainous beech forest	864 ± 303	20.87 ± 5.1	18 ± 1
1A1b	NM		1495 ± 329	36.64 ± 1.29	19 ± 2
	OG	been lorest	638 ± 84	39.14 ± 5.67	29 ± 4

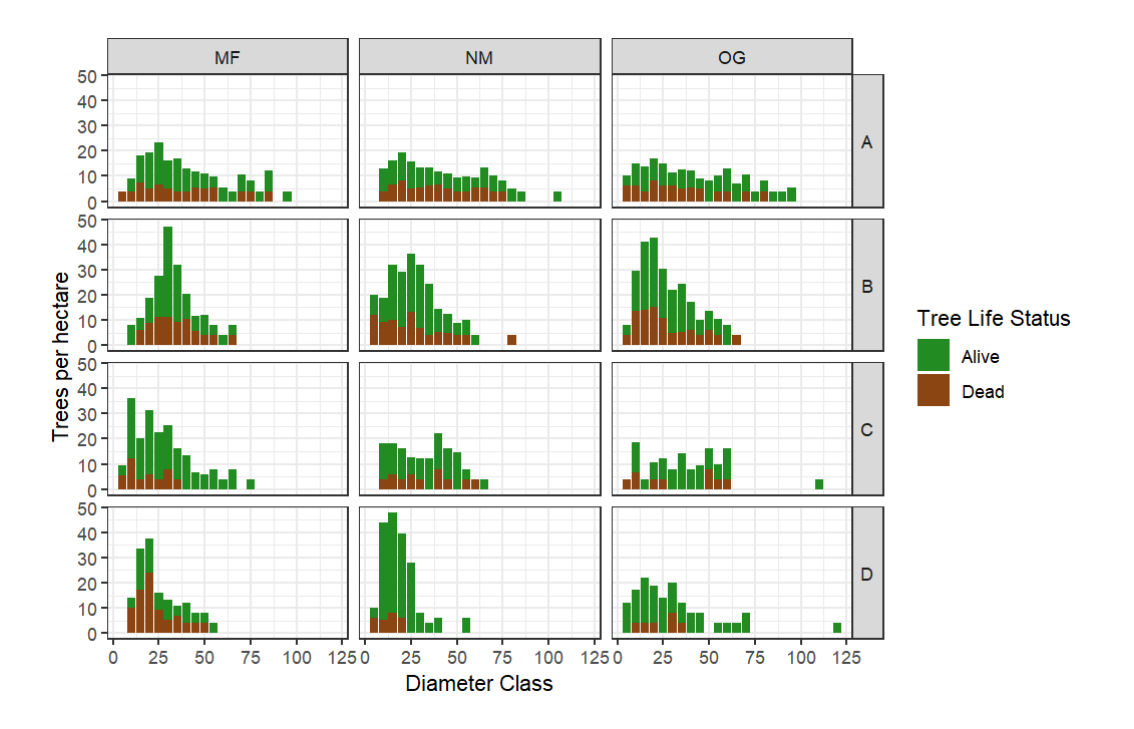


Figure 31. Mean diameter distribution of alive and dead trees by ecoregion (A = 1A2a; B = 1A2b; C = 1A2c; D = 1A1b) and time since abandonment (MF = managed forest; NM = not managed forest; OG = old-growth forest).

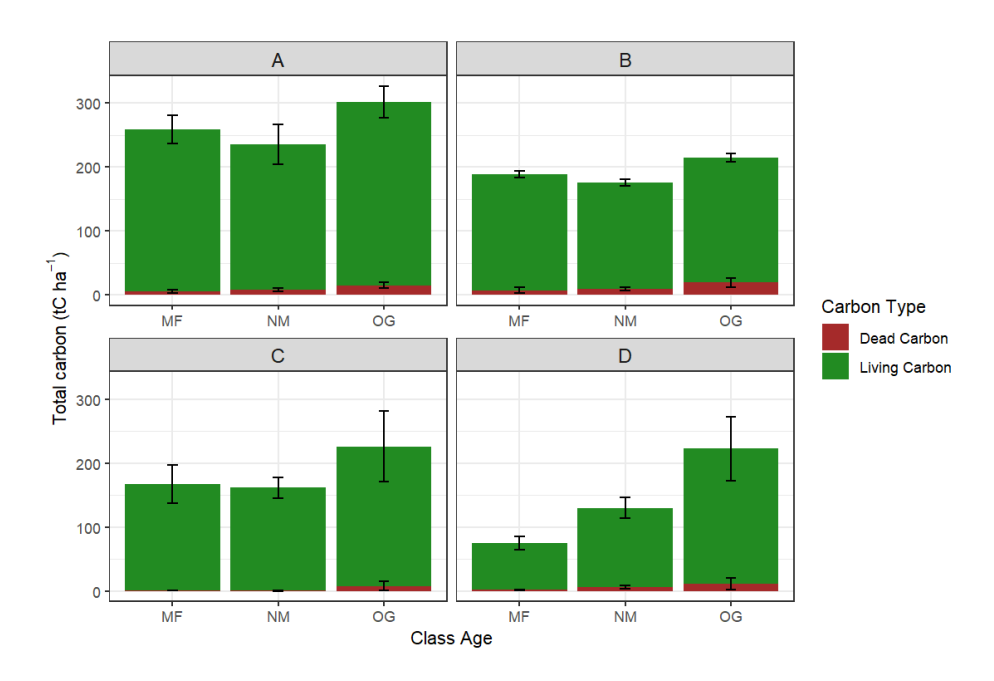


Figure 32. Total aboveground carbon stock including roots (tC ha^{-1}) by ecoregion (A =1A2a; B = 1A2b; C = 1A2c; D = 1A1b) as a function of time since abandonment (MF = managed forest; NM = not managed forest; OG = old-growth forest). Vertical bars indicate standard error.

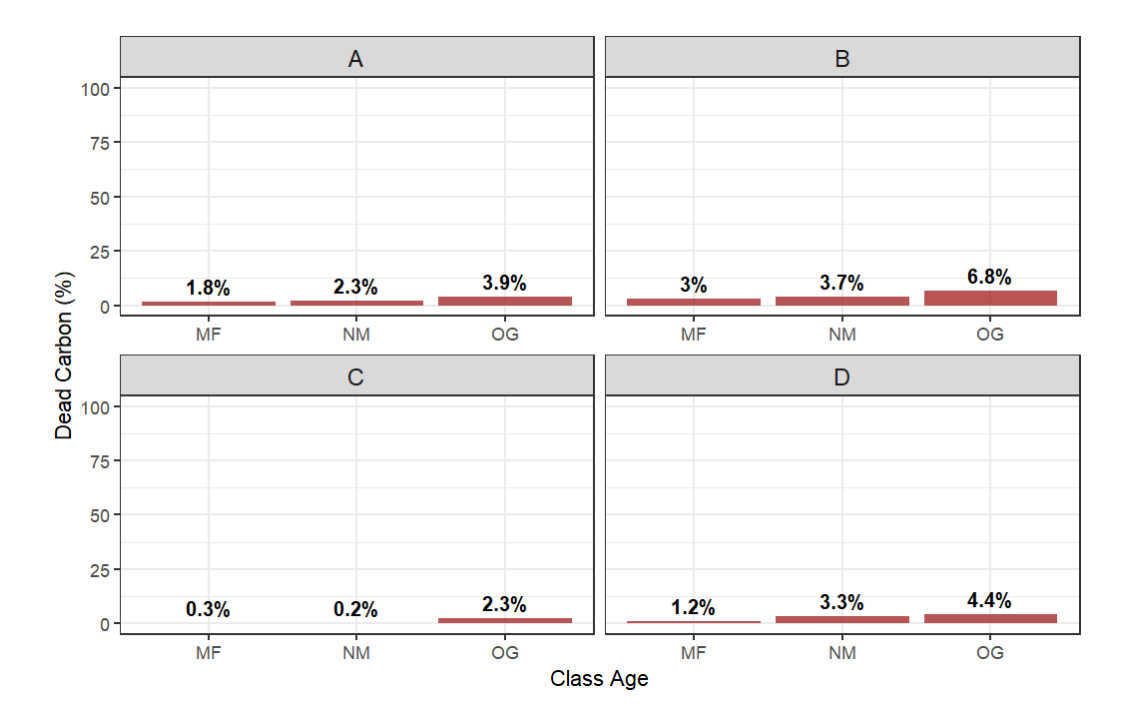


Figure 33. Proportion of carbon stock in the dead compartment (standing dead trees, snags, laying woody debris) following proforestation (MF = managed forest; NM = not managed forest; OG = old-growth forest) by ecoregion (<math>A = 1A2a; B = 1A2b; C = 1A2c; D = 1A1b).

The examined proforested sites, which exhibit substantial C stocks in both standing trees and deadwood compared to managed stands, in some cases approach the lower range of C stock benchmarks reported for old-growth forests across Europe. For instance, Keeton et al. (2010) study on Carpathian Norway spruce-silver fir old-growth forest reports a variable range of 155-165 tC ha⁻¹ for aboveground C stocks that is lower than the results of our study. Seedre et al., (2015) estimated the total C stock in a montane Norway spruce (Picea abies Karst.) old-growth forest in the Bohemian Forest (Czech Republic) at 393 ± 92 Mg C ha⁻¹. Of this, 207±59 tC ha⁻¹ ¹ (53%) was contained in living biomass, 15±9 tC ha⁻¹ (4%) in dead biomass, and 171±49 tC ha-1 (43%) in the soil. In Bialowieza core area, Matuszkiewicz et al. (2021) measured an overall C stock equal to 323 Mg C ha⁻¹ divided in 117 tC ha⁻¹ (36%) in living biomass, 20 MgC ha⁻¹ (6%) in deadwood and 186 tC ha⁻¹ (58%) in soil (up to 1 m depth). On the upper end, Motta et al. (2024) documented exceptionally higher C stocks in old-growth forests in Bosnia-Herzegovina, ranging from 398 to 484 tC ha⁻¹, representing the highest forest C sink at the continental level. Bono et al. (2024) highlighted that a considerable share (36%) of the total ecosystem C in these forest stands — including soil — is concentrated in just 5% of the largest trees. As for beech forests, total C stocks — including trees, litter layer, and mineral soil — in unmanaged stands in southern Europe range from 220 to 770 tC ha⁻¹, with an average of approximately 380 tC ha⁻¹. Tree biomass (both above- and belowground), averaging 293 tC ha⁻¹, represents the dominant C pool in these systems, accounting for between 50% and 97% of the total stock (Merino et al., 2007).

Soil C stocks

A linear mixed-effects model (LMM) was applied to log-transformed total soil C stocks to evaluate the effects of age class, ecoregion, and their interaction. The model incorporated random intercepts for location and nested plots to account for spatial structure in the data.

The results revealed significant effects of both age class and its interaction with ecoregion on log-transformed soil C. Overall, the NM (mid-successional) age class — representing stands 30–40 years after cessation of management — exhibited significantly higher soil C compared to actively managed forests (+0.67 log units, equivalent to a 95% increase; p = 0.018, Table 11). However, this positive effect was significantly moderated by ecoregion. In ecoregion 1A1b, the interaction terms showed strong negative effects for both the NM (-0.98 log units; p = 0.015) and OG (old-growth) (-1.18 log units; p = 0.046) age classes, effectively offsetting the positive age-related gains observed in ecoregion 1A2a. These findings suggest that the benefits of management abandonment on soil C stocks are ecoregion-specific and may be limited by environmental constraints or local disturbances in ecoregion 1A1b (Figure 35). The random intercepts accounted for moderate spatial variability in log-transformed soil C (location variance = 0.176; plot variance = 0.198), underscoring the importance of spatial structure. The residual variance was 0.423, and scaled residuals were well-behaved (range: -2.64 to 2.06), indicating good model fit following the log transformation.

Table 11. Results of the linear mixed-effects model (LMM) evaluating log-transformed total soil C stocks as a function of TSA, ecoregion, and their interactions. The model includes random intercepts for location and nested sampling plots to account for spatial structure. Estimates are based on REML; degrees of freedom were approximated using Satterthwaite's method. Reference levels: ecoregion = 1A2a; TSA = MF. Random effects: standard deviation of random intercepts = 0.175 (location), 0.198 (nested plot); residual SD = 0.423. Coefficients represent changes in log units; exponentiate to obtain multiplicative effects on the original scale. Significance codes: *** p < 0.001; ** p < 0.01; * p < 0.05; † p < 0.10.

Fixed Effects	Estimate	Std. Error	df	t value	p-value	Significance
Intercept	4.062	0.202	22.139	20.105	<0.001	***
Ecoregion 1A2b	0.006	0.286	22.139	0.022	0.983	
Ecoregion 1A2c	-0.016	0.286	22.139	-0.058	0.955	
Ecoregion 1A1b	0.283	0.286	22.139	0.989	0.333	
TSA NM	0.669	0.255	16.000	2.627	0.018	*
TSA OG	0.379	0.255	16.000	1.488	0.156	
Ecoregion 1A2b : TSA NM	-0.492	0.360	16.000	-1.364	0.191	
Ecoregion 1A2c : TSA NM	-0.604	0.360	16.000	-1.676	0.113	
Ecoregion 1A1b : TSA NM	-0.984	0.360	16.000	-2.731	0.015	*
Ecoregion 1A2b : TSA OG	-0.162	0.360	16.000	-0.450	0.659	
Ecoregion 1A2c : TSA OG	0.108	0.360	16.000	0.300	0.768	
Ecoregion 1A1b : TSA OG	-1.178	0.360	16.000	-3.269	0.005	**

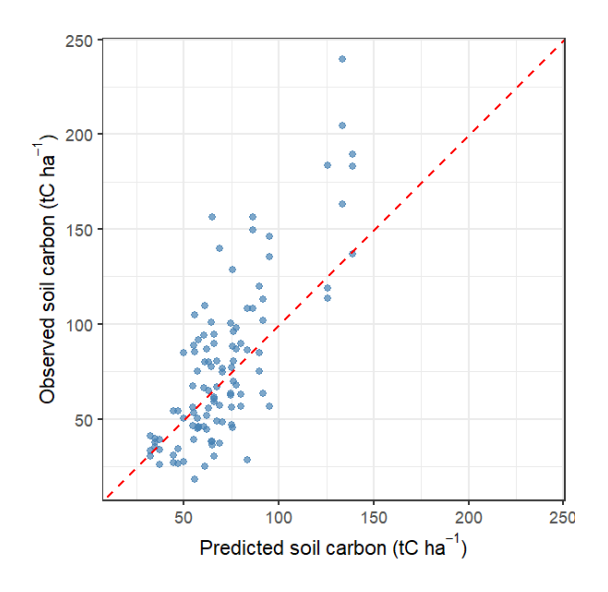


Figure 34. Comparison between predicted and observed soil C stocks.

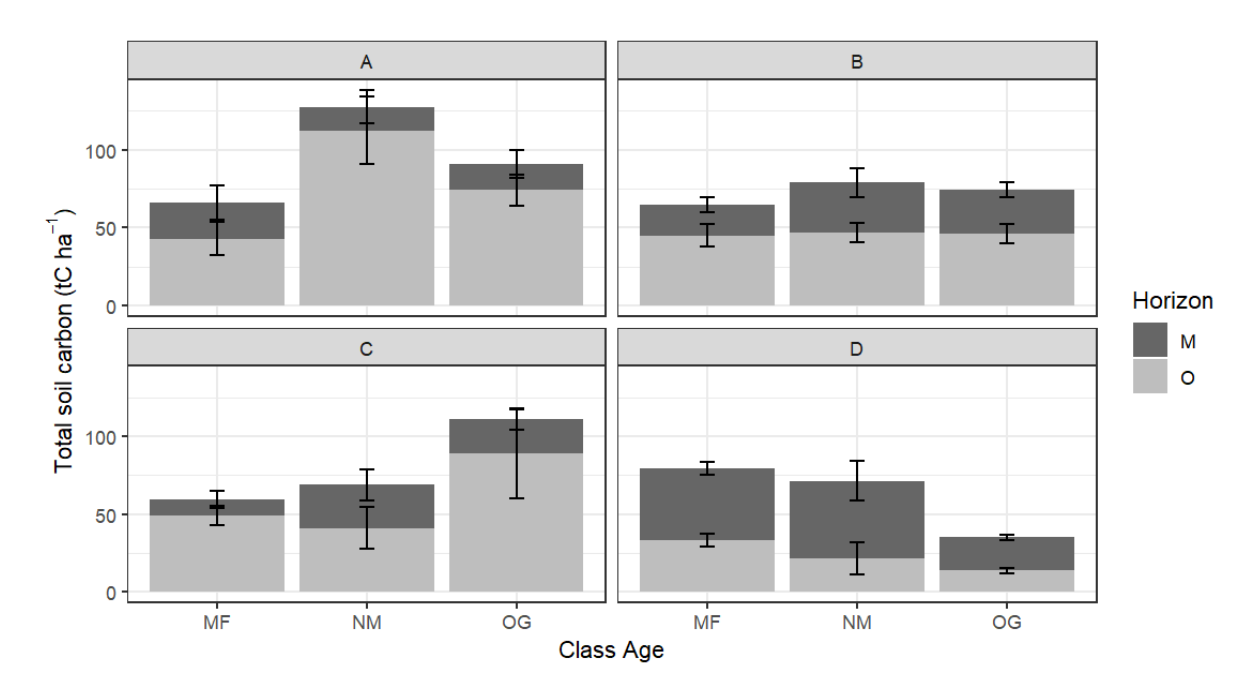


Figure 35. Total soil carbon stock (tC ha⁻¹) by horizon (M = mineral and O = organic), in different ecoregions (A = 1A2a; B = 1A2b; C = 1A2c; D = 1A1b) as a function of time since abandonment (MF = managed forest; NM = not managed forest; OG = old-growth forest). Vertical bars indicate standard error.

Ecosystem C stocks

A linear mixed-effects model accounting for variation among locations revealed that total ecosystem C stock was influenced by a combination of factors, including ecoregion, stand structure, and the interaction between TSA and ecoregion (Table 12).

In the reference condition — managed forest (TSA = 0) located in ecoregion 1A2a — the estimated total ecosystem C stock was 219.63 tC ha⁻¹, a highly significant baseline (p < 0.001). Significant differences in C stock were instead observed among ecoregions: compared to the reference ecoregion (1A2a), total ecosystem C stock was significantly lower in ecoregion 1A1b (-108.85 tC ha⁻¹, p = 0.011), and in ecoregion 1A2b (-74.77 tC ha⁻¹, p = 0.013). Ecoregion 1A2c also showed a reduction (-67.61 tC ha⁻¹), although this difference was only marginally non-significant (p = 0.102). Stand structure also played a significant role. Forests with a two-layered canopy structure stored significantly more C than multi-layered stands, with an estimated difference of +144.23 tC ha⁻¹ (p = 0.0007). Forests with a one-layered structure also showed higher C stocks compared to multi-layered ones (+57.64 tC ha⁻¹), although such a difference was not statistically significant (p = 0.119).

TSA showed no significant overall effect on total ecosystem C stock, even 60-100 years after management ceased. The estimated annual change in C since abandonment was -0.19 tC ha⁻¹ year⁻¹, but this effect was not statistically significant (p = 0.700), suggesting that, on average, TSA does not strongly affect current C levels across all the studied forests. However, the relationship between TSA and C stock varied across ecoregions. Specifically, total C stock in ecoregion 1A2c increased significantly faster with TSA than in 1A2a, with a slope of +1.42 tC ha⁻¹ year⁻¹ (p = 0.044). In contrast, differences in slopes in ecoregions 1A2b and 1A1b were smaller and not statistically significant (Table 12, Figure 36).

Table 12. Results of the linear mixed-effects model (LMM) evaluating total ecosystem carbon as a function of time since management abandonment, ecoregion, vertical structure, and their interactions. The model includes random intercepts for location to account for site-level variation. Estimates are based on REML; degrees of freedom were approximated using Satterthwaite's method. Reference levels: TSA from management = 0, Vertical structure = multi-layered, Ecoregion = 1A2a. Random effects: standard deviation of random intercepts = 28.26; residual SD = 58.90. Coefficients represent changes in tC ha⁻¹ or slope (tC ha⁻¹ year⁻¹) relative to the reference levels. Significance codes: *** p < 0.001; ** p < 0.01; * p < 0.05; † p < 0.10.

Variable	Comparison / Effect	Estimate	Std. Error	t value	p value	Significance
Intercept	1A2a, multi- layered, TSA = 0	219.63	35.98	6.10	<0.001	***
TSA from management	per year	-0.19	0.48	-0.39	0.700	
	1A2b vs 1A2a	-74.77	29.11	-2.57	0.013	*
Ecoregion	1A2c vs 1A2a	-67.61	40.64	-1.66	0.102	†
	1A1b vs 1A2a	-108.85	41.48	-2.62	0.011	*
Vertical structure	one-layered vs multi-layered	57.64	36.33	1.59	0.119	
vertical structure	two-layered vs multi-layered	144.23	40.48	3.56	0.0007	***
TSA × Ecoregion 1A2b	slope difference	0.57	0.60	0.96	0.343	
TSA × Ecoregion 1A2c	slope difference	1.61	0.78	2.07	0.044	*
TSA × Ecoregion 1A1b	slope difference	0.36	0.72	0.50	0.619	

Our findings provide nuanced insights into the factors influencing total ecosystem C stocks in post-managed forests across different Italian ecoregions. While TSA is often assumed to drive gradual C recovery (Pan et al., 2011; Zhou et al., 2006), our analysis reveals that TSA alone does not uniformly explain variation in total ecosystem C stock across the studied forests. Instead, stand structure and ecoregional differences exert a more pronounced influence, in line with emerging research on spatial heterogeneity in forest C dynamics (Keith et al., 2009).

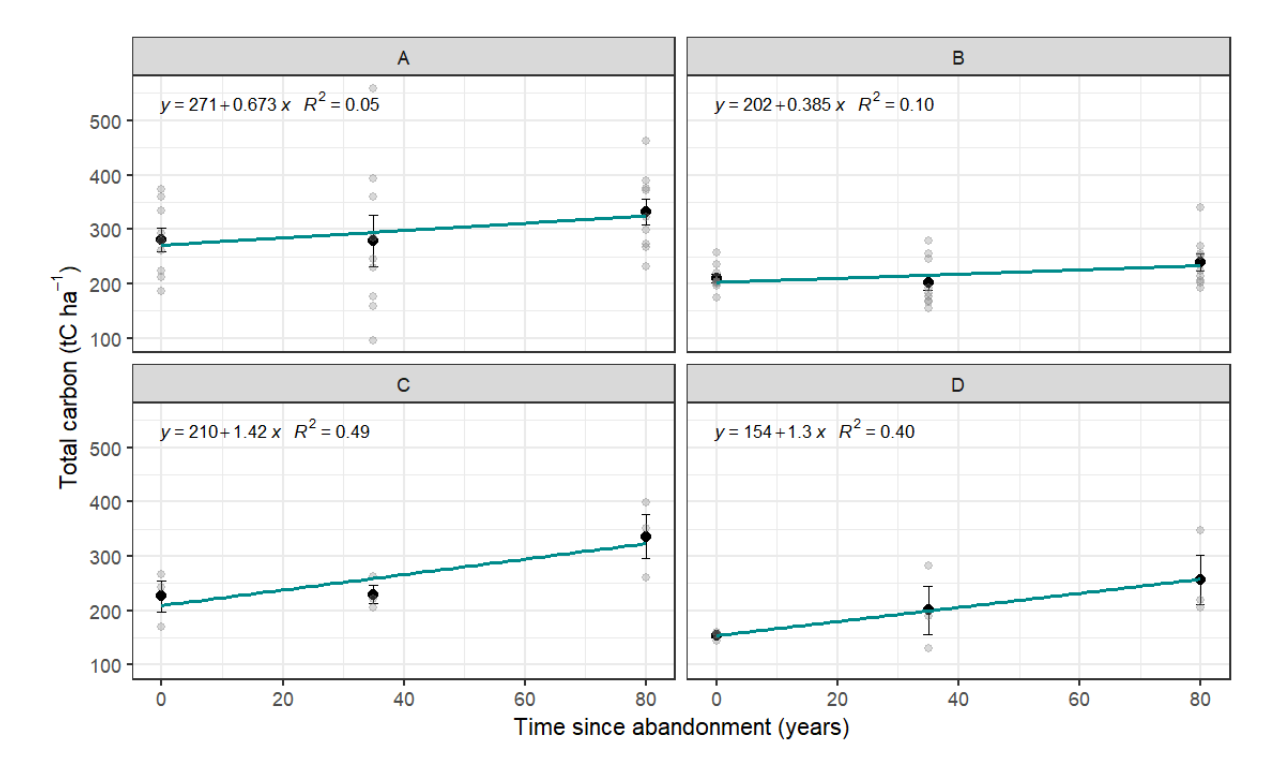


Figure 36. Total ecosystem carbon stock (tC ha^{-1}) as a function of time since abandonment, by ecoregion (A = 1A2a; B = 1A2b; C = 1A2c; D = 1A1b). Vertical bars represent standard errors.

Contrary to conventional expectations that forest C stocks increase steadily after management cessation (Keeton et al., 2011; Luyssaert et al., 2008), TSA did not have a significant overall effect on total ecosystem C, even after 60-100 years. This discrepancy may be due to C saturation in certain pools or redistribution among ecosystem components (e.g., from live biomass to deadwood and soil organic matter; Figure 37). On the contrary, the significant interaction between TSA and ecoregion, particularly in 1A2c (+1.42 tC ha⁻¹ yr⁻¹), suggests that site-specific conditions modulate the trajectory of C recovery. In contrast, ecoregions 1A1b and 1A2b did not exhibit significant increases, possibly due to lower site productivity, historical land use intensity, or slower decomposition and nutrient cycling rates. The significant baseline differences among ecoregions further highlight the importance of environmental context in shaping C storage.

Among the structural variables, canopy layering emerged as a significant determinant of ecosystem C stock. Surprisingly, two-layered forests stored significantly more C than multi-layered ones (+144.23 tC ha⁻¹, p = 0.0007), and one-layered stands also tended to store more C, albeit non-significantly. These results deviate from the commonly held view that structurally complex stands store more C due to higher vertical and horizontal diversity (Thom and Keeton, 2019; Wang et al., 2011; Yuan et al., 2018). However, this pattern may reflect differences in stand development stages: multi-layered stands in our dataset may represent structurally

complex but older or senescent stages, with a higher proportion of deadwood and lower live biomass accumulation. Alternatively, two-layered structures may indicate dynamic, unevenaged conditions with high productivity, particularly if regeneration occurs under partial canopy cover.

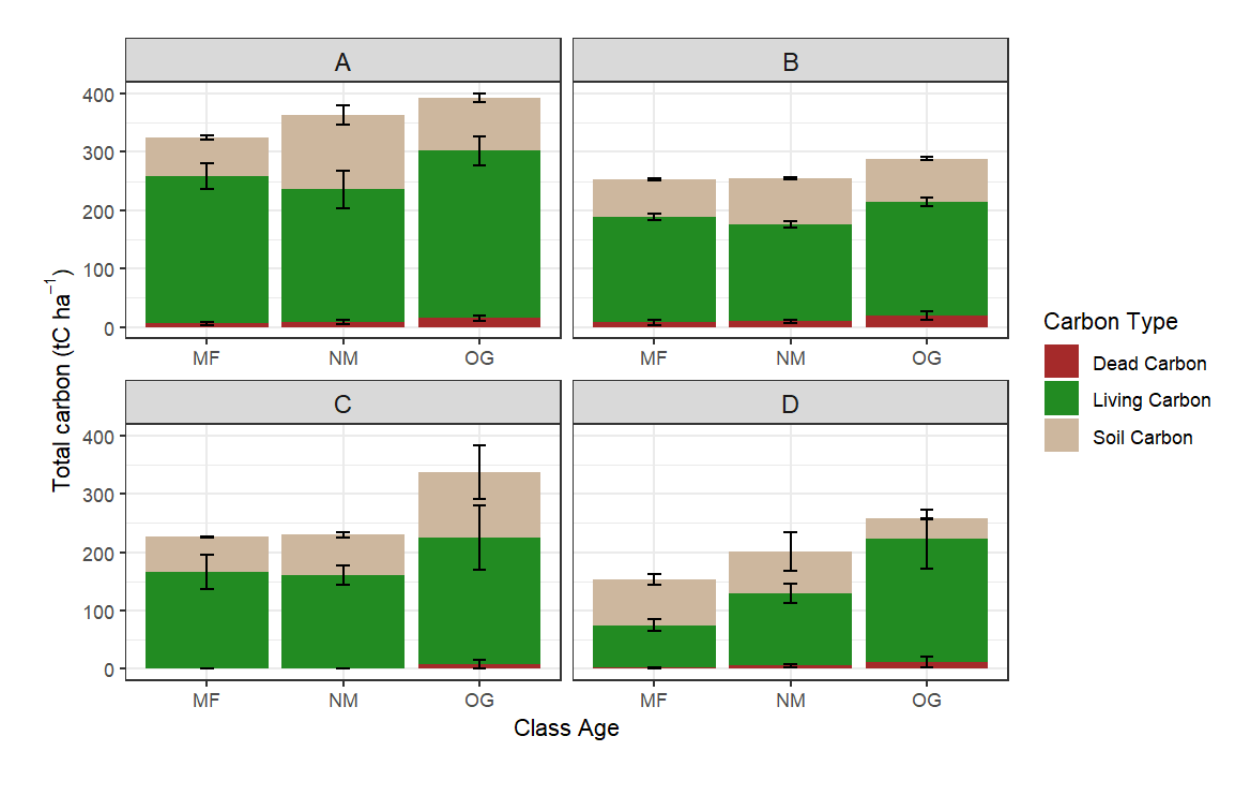


Figure 37. Partitioning of total ecosystem C in the different pools within each age class. (MF = managed forest; NM = not managed forest; OG = old-growth forest). Vertical bars indicate standard error.

These results carry important implications for proforestation strategies aimed at maximizing C storage. While proforestation advocates often assume uniform C gains in post-managed forests (Moomaw et al., 2019), our study suggests that gains are highly context-dependent. In some ecoregions, passive management can indeed lead to continued C accumulation, but in others, the legacy of past management or inherent site limitations may constrain recovery even after many decades. Therefore, spatially explicit assessments are critical for prioritizing areas where proforestation will deliver the greatest climate mitigation benefits.

7. References

- Alberti, G., Ballesteros, M., Janečkov, P., Müllerova, A., Piazza, N., Řehounková, K., Šebelíková, L., Samonil, P., A., T., 2024. Deliverable 3.1: Preliminary dataset on available carbon and biodiversity across the network. Horizon Europe Project No. 101081177, European Commission.
- Alberti, G., Peressotti, a., Piussi, P., Zerbi, G., 2008. Forest ecosystem carbon accumulation during a secondary succession in the Eastern Prealps of Italy. Forestry 81, 1–11. https://doi.org/10.1093/forestry/cpm026
- Bitunjac, D., Ostrogović Sever, M.Z., Sever, K., Merganičová, K., Marjanović, H., 2023. Dead wood volume-to-carbon conversion factors by decay class for ten tree species in Croatia and eight tree genera globally. For. Ecol. Manage. 549, 121431. https://doi.org/10.1016/J.FORECO.2023.121431
- Bono, A., Alberti, G., Berretti, R., Curovic, M., Dukic, V., Motta, R., 2024. The largest European forest carbon sinks are in the Dinaric Alps old-growth forests: comparison of direct measurements and standardised approaches. Carbon Balance Manag. 19, 1–12. https://doi.org/10.1186/s13021-024-00262-4
- Chazdon, R.L., 2013. Tropical Forest Regeneration. Encycl. Biodivers. Second Ed. 277–286. https://doi.org/10.1016/B978-0-12-384719-5.00377-4
- Chokkalingam, U., De Jong, W., 2001. Secondary forest: a working definition and typology. Int. For. Rev. 3, 19–26.
- De Cáceres, M., Casals, P., Gabriel, E., Castro, X., 2019. Scaling-up individual-level allometric equations to predict stand-level fuel loading in Mediterranean shrublands. Ann. For. Sci. 76. https://doi.org/10.1007/s13595-019-0873-4
- De Palma, A., Sanchez-Ortiz, K., Martin, P.A., Chadwick, A., Gilbert, G., Bates, A.E., Börger, L., Contu, S., Hill, S.L.L., Purvis, A., 2018. Challenges With Inferring How Land-Use Affects Terrestrial Biodiversity: Study Design, Time, Space and Synthesis. Adv. Ecol. Res. 58, 163–199. https://doi.org/10.1016/BS.AECR.2017.12.004
- EEA, 2007. European Forest Types. Categories and types for sustainable forest management, reporting and policy. Technical Report 09/2006. Copenhagen.
- Gadow, K. v., Zhang, C.Y., Wehenkel, C., Pommerening, A., Corral-Rivas, J., Korol, M., Myklush, S., Hui, G.Y., Kiviste, A., Zhao, X.H., 2012. Forest Structure and Diversity 29–83. https://doi.org/10.1007/978-94-007-2202-6_2
- Gonzalez-Akre, E., Piponiot, C., Lepore, M., Herrmann, V., Lutz, J.A., Baltzer, J.L., Dick, C.W., Gilbert, G.S., He, F., Heym, M., Huerta, A.I., Jansen, P.A., Johnson, D.J., Knapp, N., Král, K., Lin, D., Malhi, Y., McMahon, S.M., Myers, J.A., Orwig, D., Rodríguez-Hernández, D.I., Russo, S.E., Shue, J., Wang, X., Wolf, A., Yang, T., Davies, S.J., Anderson-Teixeira, K.J., 2022. allodb: An R package for biomass estimation at globally distributed extratropical forest plots. Methods Ecol. Evol. 13, 330–338. https://doi.org/10.1111/2041-210X.13756
- Guidi, C., Vesterdal, L., Gianelle, D., Rodeghiero, M., 2014. Changes in soil organic carbon and nitrogen following forest expansion on grassland in the Southern Alps. For. Ecol. Manage. 328, 103–116. https://doi.org/10.1016/j.foreco.2014.05.025
- Guo, L.B., Gifford, R.M., 2002. Soil carbon stocks and land use change: A meta analysis. Glob. Chang. Biol. 8, 345–360. https://doi.org/10.1046/j.1354-1013.2002.00486.x

- Harmon, M.E., Sexton, J., Brook, H., 1996. GUIDELINES FOR MEASUREMENTS OF WOODY DETRITUS IN FOREST ECOSYSTEMS.
- IPCC, 2006. Guidelines for National Greenhouse Gas Inventories Agriculture, Forestry and Other Land Use (volume 4).
- IPCC, 2003. Good Practice Guidance for Land Use, Land-Use Change and Forestry.
- IPCC, 2000. Land use, land use change and forestry. Cambridge University Press.
- Jackson, R., Banner, J., Jobbagy, E., Pockman, W., Wall, D., 2002. Ecosystem carbon loss with woody plant invasion of grasslands. Nature 418, 623–626.
- Keeton, W.S., Chernyavskyy, M., Gratzer, G., Main-Knorn, M., Shpylchak, M., Bihun, Y., 2010. Structural characteristics and aboveground biomass of old-growth spruce-fir stands in the eastern Carpathian mountains, Ukraine. Plant Biosyst. 144, 148–159. https://doi.org/10.1080/11263500903560512
- Keeton, W.S., Whitman, A.A., McGee, G.C., Goodale, C.L., 2011. Late-Successional Biomass Development in Northern Hardwood-Conifer Forests of the Northeastern United States. For. Sci. 57, 489–505. https://doi.org/10.1093/FORESTSCIENCE/57.6.489
- Keith, H., Mackey, B.G., Lindenmayer, D.B., 2009. Re-evaluation of forest biomass carbon stocks and lessons from the world's most carbon-dense forests. Proc. Natl. Acad. Sci. U. S. A. 106, 11635–11640. https://doi.org/10.1073/PNAS.0901970106/SUPPL FILE/0901970106SI.PDF
- Laganière, J., Angers, D.A., Paré, D., 2010. Carbon accumulation in agricultural soils after afforestation: A meta-analysis. Glob. Chang. Biol. 16, 439–453. https://doi.org/10.1111/j.1365-2486.2009.01930.x
- Luyssaert, S., Schulze, E.D., Börner, A., Knohl, A., Hessenmöller, D., Law, B.E., Ciais, P., Grace, J., 2008. Old-growth forests as global carbon sinks. Nature 455, 213–215. https://doi.org/10.1038/nature07276
- Matuszkiewicz, J.M., Affek, A.N., Kowalska, A., 2021. Current and potential carbon stock in the forest communities of the Białowieża Biosphere Reserve. For. Ecol. Manage. 502, 119702. https://doi.org/10.1016/J.FORECO.2021.119702
- Merino, A., Real, C., Álvarez-González, J.G., Rodríguez-Guitián, M.A., 2007. Forest structure and C stocks in natural Fagus sylvatica forest in southern Europe: The effects of past management. For. Ecol. Manage. 250, 206–214. https://doi.org/10.1016/J.FORECO.2007.05.016
- Moomaw, W.R., Masino, S.A., Faison, E.K., 2019. Intact Forests in the United States: Proforestation Mitigates Climate Change and Serves the Greatest Good. Front. For. Glob. Chang. 2, 1–10. https://doi.org/10.3389/ffgc.2019.00027
- Motta, R., Alberti, G., Ascoli, D., Keren, S., Meloni, F., Ruffinatto, F., Nola, P., 2024. Old-growth forests in the Dinaric Alps of Bosnia-Herzegovina and Montenegro: a continental hot-spot for research and biodiversity. Front. For. Glob. Chang. 1–16. https://doi.org/10.3389/ffgc.2024.1371144
- Nezhad, M., Gajski, D., Jeanroy, C., Verburg, P., Alberti, G., Samonil, P., n.d. Soil organic carbon dynamics in rewilded abandoned lands across Europe: current status and knowledge gaps. Sci. Total Environ.
- Pan, Y., Birdsey, R.A., Fang, J., Houghton, R.A., Kauppi, P.E., Kurz, W.A., Phillips, O.L., Shvidenko, A., Lewis, S.L., Canadell, J.G., Ciais, P., Jackson, R.B., Pacala, S.W., McGuire, A.D., Piao, S., Rautiainen, A., Sitch, S., Hayes, D., Canadell, J.G., Khatiwala,

- S., Primeau, F., Hall, T., Quéré, C. Le, Dixon, R.K., Kauppi, P.E., Kurz, W.A., Stinson, G., Rampley, G.J., Dymond, C.C., Neilson, E.T., Stinson, G., Birdsey, R.A., Pregitzer, K., Lucier, A., Kauppi, P.E., Pan, Y., Pan, Y., Birdsey, R.A., Hom, J., McCullough, K., Mantgem, P.J. van, Breshears, D.D., Ciais, P., Fang, J., Chen, A., Peng, C., Zhao, S., Ci, L., Lewis, S.L., Phillips, O.L., Gloor, M., Lewis, S.L., Lloyd, J., Sitch, S., Mitchard, E.T.A., Laurance, W.F., Houghton, R.A., Friedlingstein, P., Tarnocai, C., Hooijer, A., Page, S.E., Rieley, J.O., Banks, C.J., McGuire, A.D., Goodale, C.L., Sarmiento, J.L., Schulze, E.D., Pacala, S.W., Phillips, O.L., Metsaranta, J.M., Kurz, W.A., Neilson, E.T., Stinson, G., Zhao, M., Running, S.W., Houghton, R.A., 2011. A large and persistent carbon sink in the world's forests. Science (80-.). 333, 988–993. https://doi.org/10.1126/science.1201609
- Paul, K.I., Polglase, P.J., Nyakuengama, J.G., Khanna, P.K., 2002. Change in soil carbon following afforestation. For. Ecol. Manage. 168, 241–257.
- Prescott, C.E., 2002. The influence of the forest canopy on nutrient cycling. Tree Physiol. 22, 1193–1200. https://doi.org/10.1093/TREEPHYS/22.15-16.1193,
- Risch, A.C., Jurgensen, M.F., Page-Dumroese, D.S., Wildi, O., Schütz, M., 2008. Long-term development of above- and below-ground carbon stocks following land-use change in subalpine ecosystems of the Swiss National Park. https://doi.org/10.1139/X08-014 38, 1590–1602. https://doi.org/10.1139/X08-014
- Seedre, M., Kopáček, J., Janda, P., Bače, R., Svoboda, M., 2015. Carbon pools in a montane old-growth Norway spruce ecosystem in Bohemian Forest: Effects of stand age and elevation. For. Ecol. Manage. 346, 106–113. https://doi.org/10.1016/j.foreco.2015.02.034
- Thom, D., Keeton, W.S., 2019. Stand structure drives disparities in carbon storage in northern hardwood-conifer forests. For. Ecol. Manage. 442, 10–20. https://doi.org/10.1016/J.FORECO.2019.03.053
- Thuille, A., Schulze, E.D., 2006. Carbon dynamics in successional and afforested spruce stands in Thuringia and the Alps. Glob. Chang. Biol. 12, 325–342. https://doi.org/10.1111/J.1365-2486.2005.01078.X
- Vesterdal, L., Clarke, N., Sigurdsson, B.D., Gundersen, P., 2013. Do tree species influence soil carbon stocks in temperate and boreal forests? For. Ecol. Manage. 309, 4–18. https://doi.org/10.1016/j.foreco.2013.01.017
- Wang, W., Lei, X., Ma, Z., Kneeshaw, D.D., Peng, C., 2011. Positive Relationship between Aboveground Carbon Stocks and Structural Diversity in Spruce-Dominated Forest Stands in New Brunswick, Canada. For. Sci. 57, 506–515. https://doi.org/10.1093/FORESTSCIENCE/57.6.506
- Yuan, Z., Wang, S., Ali, A., Gazol, A., Ruiz-Benito, P., Wang, X., Lin, F., Ye, J., Hao, Z., Loreau, M., 2018. Aboveground carbon storage is driven by functional trait composition and stand structural attributes rather than biodiversity in temperate mixed forests recovering from disturbances. Ann. For. Sci. 75, 1–13. https://doi.org/10.1007/S13595-018-0745-3/FIGURES/3
- Zhou, G., Liu, S., Li, Z., Zhang, D., Tang, X., Zhou, C., Yan, J., Mo, J., 2006. Old-growth forests can accumulate carbon in soils. Science (80-.). 314, 1417. https://doi.org/10.1126/SCIENCE.1130168/SUPPL_FILE/ZHOU.SOM.PDF